# *IN VIVO CELL TRACKING USING NON-INVASIVE IMAGING OF PARAMAGNETIC/SUPERPARAMAGNETIC PARTICLES WITH PARTICULAR RELEVANCE FOR CELL-BASED TREATMENTS OF NEUROLOGICAL AND CARDIAC DISEASES*

Joel C. Glover[1,2], Markus Aswendt*[3], Jean-Luc Boulland*[1,2], Jasna Lojk*[4], Stefan Stamenković*[5], Pavle Andjus[5], Fabrizio Fiori[6], Mathias Hoehn[3], Dinko Mitrecic[7], Mojca Pavlin[4,8], Stefano Cavalli[9], Caterina Frati[9], Federico Quaini[9], on behalf of the EU COST Action 16122 (BIONECA)

*contributed equally

**Running title:** Non-invasive in vivo cell tracking

**Manuscript category:** Review

**Affiliations:**

1 Laboratory for Neural Development and Optical Recording (NDEVOR), Department of Molecular Medicine, Institute of Basic Medical Sciences, University of Oslo, PB 1105 Blindern, Oslo, Norway

2 Norwegian Center for Stem Cell Research, Oslo University Hospital, Oslo, Norway

3 Institut für Neurowissenschaften und Medizin, Forschungszentrum Jülich, Leo-Brandt-Str. 5, 52425 Jülich, Germany

4 Group for Nano and Biotechnological Applications, Faculty of Electrical Engineering, University of Ljubljana, Trzaska cesta 25, Ljubljana, Slovenia

5 Center for Laser Microscopy, Dept of Physiology and Biochemistry, Faculty of Biology, University of Belgrade, PB 52, 11001 Belgrade, Serbia

6 Department of Applied Physics, Università Politecnica delle Marche - Di.S.C.O., Via Brecce Bianche
60131 Ancona, Italy

7 Laboratory for Stem Cells, Croatian Institute for Brain Research, School of Medicine, University of Zagreb, Croatia

8 Institute of Biophysics, University of Ljubljana, Faculty of Medicine, Vrazov trg 2, Ljubljana, Slovenia

9 Department of Medicine and Surgery, University of Parma, Italy

**Table of contents**

**Abbreviations:**

*BBB (blood-brain barrier)*

*bMPIO (biodegradable micrometer-sized particle of iron oxide)*

*ESC (embryonic stem cell)*

*MEIO (magnetism-engineered iron oxide nanoparticle)*

*MION (monocrystalline iron oxide nanocompound)*

*MPIO (micrometer-sized particle of iron oxide)*

*MRI (magnetic resonance imaging)*

*MSC (mesenchymal stem cell)*

*NPC (neural progenitor cell)*

*NSC (neural stem cell)*

*PP/SPP (paramagnetic/superparamagnetic particle)*

*SPIO (superparamagnetic particle of iron oxide)*

*SPION (superparamagnetic iron oxide nanoparticle)*

*USPIO (ultrasmall superparamagnetic particle of iron oxide)*

*VSOP (very small superparamagnetic iron oxide particles)*

**0. Abstract**

*Purpose*: Stem cell-based therapeutics is a rapidly developing field associated with a number of clinical challenges. One such challenge lies in the implementation of methods to track stem cells and stem cell-derived cells in experimental animal models and in the living patient. Here we provide an overview of cell tracking in the context of cardiac and neurological disease, focusing on the use of paramagnetic and superparamagnetic particles (PP/SPPs) that can be visualized *in vivo* using magnetic resonance imaging (MRI).

*Procedures*: Critical assessment of scientific literature.

*Results*: We discuss the types of PP/SPPs available for such tracking, their advantages and limitations, approaches for labeling cells with PP/SPPs, biological interactions and effects of PP/SPPs at the molecular and cellular levels, and MRI-based and associated approaches for *in vivo* and histological visualization. We conclude with reviews of the literature on PP/SPP-based cell tracking in cardiac and neurological disease, covering both preclinical and clinical studies.

*Conclusions*: Developing cellular labeling approaches with PP/SPPs has become an important area of research aimed at providing valid cell tracking in patients. As the development of PP/SPPs and their *in vivo* imaging advances, and assuming remaining issues can be resolved, we expect that their clinical use in cardiological and neurological disease will become a reality. Non-invasive imaging of PP/SPP-labeled cells will then become an important tool in assessing and controlling cell implantation therapies.

**I. Introduction**

The use of stem cells in regenerative medicine holds the promise of enabling the repair of tissues and organs, either directly through the replacement of cells lost due to acute injury or neurodegeneration, or indirectly through anti-inflammatory and growth-promoting mechanisms. Stem cell-based regenerative therapies are especially relevant in the case of tissues with low regenerative capabilities, such as cardiac and central nervous system (CNS) tissue (Uygur and Lee 2016; Winner and

Winkler 2015). A number of studies have investigated the potential of delivering cells to the heart and CNS either through direct stereotactic injection or indirect delivery via the circulatory system or subdural space (Tuszynski et al 2014; Rafatian et al 2018). In both scenarios, transplanted cells migrate towards the site of injury, potentially attracted by released cytokines. From a clinical perspective, it is necessary to develop methods to locate and track human stem cells with high precision, dynamically and noninvasively after transplantation (Aarntzen et al 2012; Srivastava and Bulte 2014).

Labelling cells to permit *in vivo* visualization is important for localizing the cells, tracking their migration within tissues and confirming their engraftment into target areas. During the development of a cell-based therapy, cell labelling and tracking facilitates the determination of the optimal cell number and administration route, the engrafting efficiency and on-target and potential off-target accumulation. All of these features are important in assessing both the therapeutic efficacy and the safety of the cell therapy (Cromer Berman et al. 2011).

Fluorescent or luminescent markers permit cell tracking in the whole animal at relatively low spatial resolution (Contag and Bachmann 2002) or at higher resolution but with depth limitations (<500 µm) (Helmchen and Denk 2005). To overcome depth constraints, radiochemical tracking methods based on PET (positron emission tomography) or SPECT (single photon emission computed tomography) and magnetic tracking methods using MRI (magnetic resonance imaging) have been developed. Visualization depth for PET and SPECT is unlimited, but spatial resolution remains modest, around 1–2 mm (Jacobs and Cherry 2001). Although considered less sensitive than PET at the molecular level, MRI of paramagnetic and superparamagnetic markers can achieve substantially higher spatial resolution, depending on the field strength of the magnet used (deKemp et al 2010). Like PET and SPECT, MRI is also essentially depth-unlimited but does not require the production of expensive radiochemical compounds or involve potentially harmful radiation load during long-term tracking. Thus, MRI of cells labeled with paramagnetic or superparamagnetic particles provides important advantages as a

tool for cell tracking (Long et al 2009; Li et al 2010). Since the first demonstration of MRI-based stem cell tracking *in vivo* by Hoehn et al. in 2002 (Hoehn et al., 2002), the technique has been improved to detect transplanted stem cells for weeks, months and up to one year in rodents (Modo et al., 2009; Modo et al., 2004; Wen et al., 2014).

In this review, we focus on the potential for utilizing paramagnetic and superparamagnetic particles (we use hereafter the abbreviation PP/SPPs to designate these collectively) to label and track cells non-invasively following introduction into living organisms. We address the available types of PP/SPPs and their properties, the visualization modalities that can be used for non-invasive tracking, a brief account of auxiliary cell labelling agents, the effects of PP/SPPs on molecular and cellular processes, and an overview of already published preclinical and clinical utilization of PP/SPPs in the context of cardiac and neurological disease.

## II. Methodological background

### A. Types of paramagnetic and superparamagnetic particles

Paramagnetism is exhibited by a number of metals and metal-containing compounds, but iron oxide is typically used for biomedical applications on account of its biocompatibility, low toxicity, low cost, and high detection sensitivity. PP/SPPs of iron oxide are typically categorized according to their size, magnetic properties and coatings. A number of these are commercially available, and some have been approved by the FDA for internal use in clinical applications, in many cases as contrast agents. The size of PP/SPPs impacts on both the feasibility of cell loading and the facility of detection by MRI. In general, there can be limits to the size of PP/SPPs that a given cell type can engulf, but on the other hand, the larger the PP/SPP, the higher the density of paramagnetic material and thus the more easily detected.

The size range of PP/SPPs includes partly overlapping categories and types (Figure 1) with a variety of established names: magnetism-engineered iron oxide (MEIO)

nanoparticles (6–12 nm), monocrystalline iron oxide nanocompounds (MIONs, 5–20 nm), ultrasmall superparamagnetic iron oxide particles (USPIOs, 30–50 nm), and nanometer-sized superparamagnetic iron oxide particles (SPIOs, 50–150 nm), all of which permit visualization of cell clusters or single cells of types that can engulf very high particle loads, such as macrophages (Lee et al 2007, Shen et al 1993). At the upper end of the size spectrum are the micrometer-sized particles of iron oxide (MPIOs, one to several microns in diameter), which are more readily detected at single cell resolution than the smaller particles of iron oxide due to the higher density of iron they provide (Heyn et al 2006; Shapiro et al 2006). Some PP/SPPs have been fabricated with different types of coatings to enable functionalization with surface molecules (Shubayev et al 2009, Masserini 2013). In addition, biodegradable forms have been fabricated to facilitate clinical use, based on polymer encapsulated metallic nanocrystal clusters, rather than polymer coated single iron oxide cores (Nkansah et al 2011, Shapiro 2015). Another platform for formulating PP/SPPs is in the form of magnetoliposomes, which can be used for visualization and/or drug delivery as well as induction of targeted magnetic fluid hyperthermia for ablating cells (reviewed in Monnier et al 2014). Detection limits for visualization of PP/SPPs depend on the type, but the mean mass of iron required per cell is generally in the range of 3-30 pg (Shapiro et al 2006).

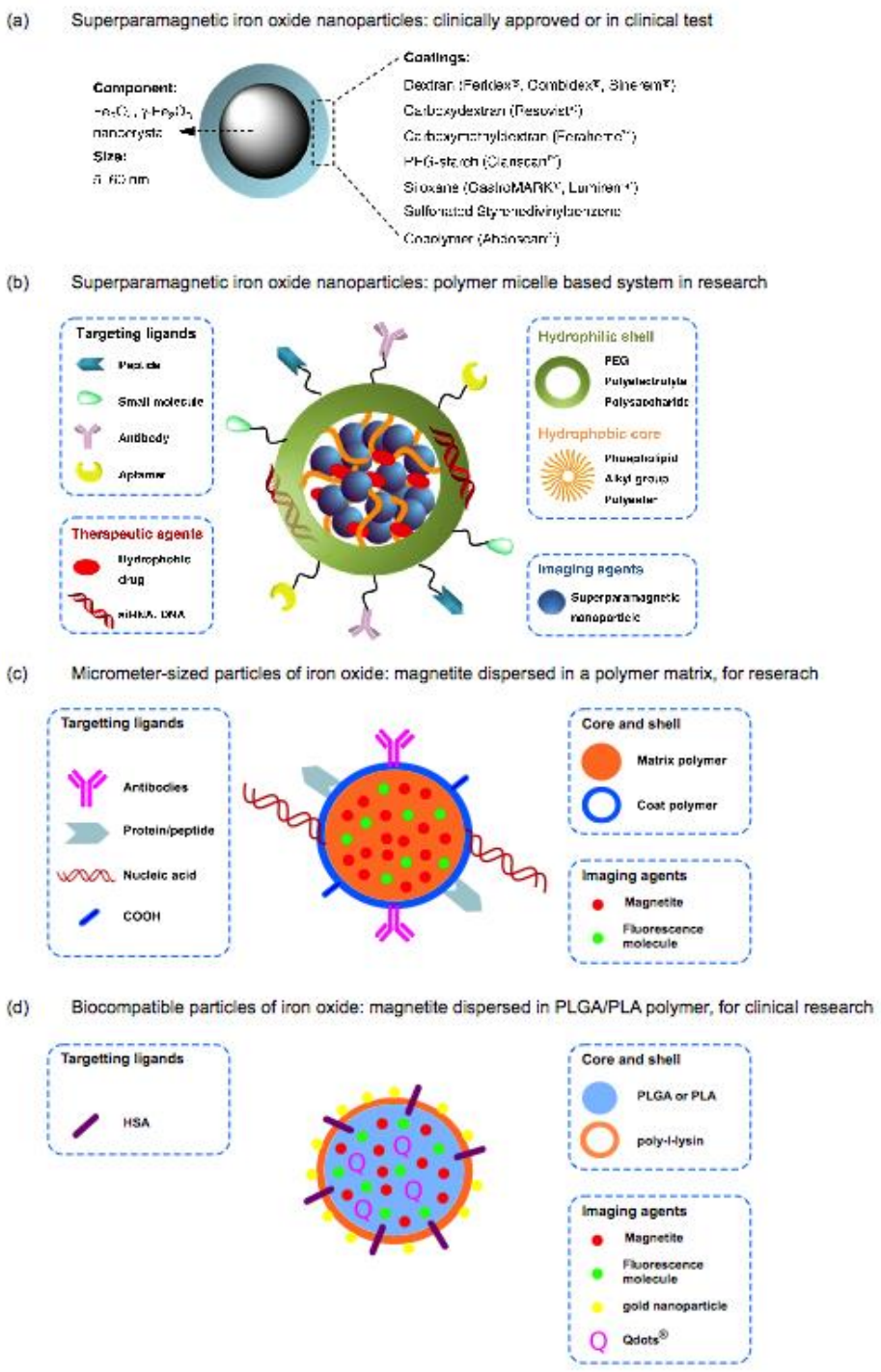


*Figure 1. Size range and functionalization possibilities for PP/SPPs. Panels a and b from Jin et al (2014), with permission. Include scale bars to indicate relative sizes of particles.*

## B. Modes of delivery

### 1. Pre-implantation *in vitro* cell loading

The main advantages of loading cells *in vitro* prior to implantation (Barrow et al. 2015) are that labelling is restricted (at least initially, see below) to the implanted cells and a considerably smaller amount of PP/SPPs is introduced into the body, reducing potential adverse effects and toxicity. *In vitro* loading is usually achieved by suspension of PP/SPPs in cell culture medium (Yeh et al. 1993, 1995; Lojk et al. 2015). Internalization occurs through intrinsic endocytic pathways and leads to accumulation of PP/SPPs inside the cells.

Uptake rate and capacity depend on the physico-chemical properties of PP/SPPs and their coating, but also on the properties of the selected cell type. Whereas certain cell types, like macrophages, can internalize PP/SPPs in large quantities, the uptake rate exhibited by other cell types may be lower, creating detection issues after implantation. To increase uptake, the surface of PP/SPPs can be modified with transfection agents, amine moieties or cell-penetrating peptides. The most commonly used transfection agents are poly-L-lysine and protamine sulphate, which have low cell toxicity at doses required for internalization (Josephson et al. 1999; Lewin et al. 2000; Hoehn et al. 2002; Kraitchman et al. 2003; Frank et al. 2003; Arbab et al. 2003b, 2004; Thu et al. 2009)(Küstermann et al 2008). Physical methods can also be used to augment cell-intrinsic uptake mechanisms. Electroporation (Walczak et al. 2005, 2006), ultrasound (Qiu et al. 2010; Xie et al. 2010) and microinjection both bypass the intrinsic cellular uptake mechanisms and provide immediate loading of PP/SPPs, avoiding prolonged *in vitro* incubation, which might influence later cell behavior. PP/SPPs can also be attached to the cell surface using antibodies or other molecules that target specific cell surface markers (Bulte et al 1999; Ahrens et al 2003; Shapiro 2007), but this tends to result in lower PP/SPP content per cell and risks recognition of the cells by the immune system (Lewin et al. 2000). Moreover, surface markers change and redistribute as cells differentiate, migrate and function, which can result in loss of labelling.

Regardless of the loading method used, the amount of loaded PP/SPPs must reach the minimal amount required for detection and must not adversely affect cell viability or cell functions such as migration, engrafting and differentiation. Whereas most studies do not report major toxicological effects on different types of stem cells and other cell types following labeling with PP/SPPs at concentrations sufficient for efficient cell labelling (Hill et al. 2003; Arbab et al. 2004, 2005b; Boulland et al 2012; Detante et al. 2012; Shen et al. 2013), certain PP/SPP types have been shown to impair cell differentiation and migration in some cell types. Feridex nanoparticles, for example, have been shown to inhibit chondrogenesis, but not adipogenesis or osteogenesis (Kostura et al. 2004; Bulte et al. 2004). Feracabotran nanoparticles have been shown to inhibit mesenchymal stem cell differentiation, but promote migration (Chen et al. 2010). A decrease of phagocytotic capacity, an increase in migration and apoptosis and several biochemical alterations have been reported in PP/SPP-loaded macrophages *in vitro*, changes that might impede pathogen removal and immune responses *in vivo* (Hsiao et al. 2008; Lunov et al. 2010a). Studies performed on neural stem cells have so far indicated no adverse effects of PP/SPPs on cell survival, migration, differentiation or electrophysiological characteristics (Bulte et al. 2001; Guzman et al. 2007; Focke et al. 2008; Cohen et al. 2010; Boulland et al 2012; Shen et al. 2013; Ramos-Gómez et al. 2015; Goodfellow et al. 2016). Similarly, no adverse effects on cell viability, physiology, differentiation or engraftment abilities have been reported for ESC-derived cardiomyocytes loaded with PP/SPPs (Au et al. 2009). Ideally, the effects of PP/SPPs on cell differentiation and behavior should be characterized *in vitro* and in animal models for each combination of PP/SPP and cell type prior to use as a tool for *in vivo* tracking.

## 2. *In vivo* delivery

### a. Intravenous injection

The fate of intravenously injected PP/SPPs depends on their size. Particles larger than a few microns in diameter will to a great extent be trapped in the capillaries of the lungs, and in other capillary systems beyond. Smaller particles, like SPIONs, pass the lungs but are rapidly taken up by cells of the reticuloendothelial system in the liver and spleen, leading to rapid clearance from the circulatory system. Smaller

USPIOs have been shown to have longer circulation times and are more readily taken up by phagocytic cells in blood and lymph nodes. Accordingly, USPIO agents such as Ferumoxtran-10 (Combidex, Sinerem) are in advanced clinical development for lymph node imaging whereas SPIO particles such as ferumoxide (Endorem, Resovist) have been approved by the FDA for liver imaging (Wang YJ 2011).

**b. Delivery via preloaded macrophages**

Macrophages are attracted to sites of tissue damage and inflammation and to tumors through chemotactic mechanisms (Fujiwara and Kobayashi 2005) (Bajetto et al. 2006) (Kaminski et al 2012, Chanmee et al 2014), and thus can be used to localize such targets *in vivo* if they are labeled with PP/SPPs and injected either in the vicinity of tissue damage or intravenously. For example, MPIO-labeled murine macrophages have been injected intravenously into rats with brain gliomas and shown to target the brain tumor, as monitored by MRI and confirmed by post mortem histology (Valable et al. 2008). In another example, pre-labeled, intracerebrally or intravenously injected monocytes have been shown to infiltrate into ischemic territories in the brain (Selt et al., 2016).

**c. Direct delivery into the brain**

***Via the blood-brain barrier***. The blood-brain barrier (BBB) is a semipermeable barrier created by endothelial cells, pericytes, and astrocytic endfeet, and regulates the traffic of substances between blood and brain (Sharma 2009). Several studies have shown that PP/SPPs in general penetrate the intact BBB poorly, but that penetration can potentially be facilitated by combination with lipophilic carriers or surfactants such as polysorbates (Saiyed et al 2010, Yuan et al 2015) or by magnetic force-mediated dragging (Kong et al 2012, Thomsen et al 2013, Busquets et al 2015). Penetration is also increased through BBB that is damaged or compromised, for example by neurodegenerative disease or age (Yarjanli et al. 2017) (Cengelli et al 2006). The BBB can also be damaged by PP/SPPs themselves, which thus facilitate their own delivery into the brain (Imam et al. 2015). Desestret et al (2009) analyzed the changes in MRI signal following post-injury intravenous injection of the USPIO Furumoxtran-10 (Sineren) into a mouse model of stroke (cerebral artery occlusion).

They followed PP/SPP accumulation in the brain with MRI and histologically confirmed the presence of PP/SPPs in areas of detected MR signal. They showed that PP/SPPs reached the brain mainly by passive diffusion through the BBB at sites of PP/SPP-induced damage rather than being taken up by infiltrating peripheral phagocytes (Desestret et al. 2009). Exploiting the ability of PP/SPPs to damage the BBB is, however, a risky proposition, since a damaged BBB will also allow passage of other potentially harmful blood-borne substances into the brain.

Delivery of PP/SPPs through the BBB can also be enhanced by receptor-mediated transcytosis. To enable this, PP/SPPs can be conjugated or coated with specific ligands (such as insulin, transferrin, lactoferrin, ceruloplasmin, apolipoproteins, diphtheria toxin) that bind to receptors present on the endothelial cell surface. Ligand-conjugated PP/SPPs are then endocytosed, moved to the opposite pole of the endothelial cell and exocytosed on the abluminal side. In an *in vitro* model of BBB, endocytosis of transferrin-coated polylactide-co-glycolide PP/SPPs via the caveolae-mediated endocytic pathway was about 20-fold greater than that of uncoated PP/SPPs (Chang et al. 2009). Similarly, lactoferrin-receptor mediated endocytosis was used for internalization of lactoferrin-coated Fe3O4 PP/SPPs *in vivo* and *in vitro* (Qiao et al. 2012). PP/SPPs can also be loaded into monocytes/macrophages, which can cross the BBB in instances of brain inflammation.

***Via olfactory epithelium***. Another possible delivery route to the brain involves intranasal application to the olfactory epithelium, which delivers PP/SPPs to the brain through anterograde olfactory axonal transport (Wang et al. 2008), thus bypassing the BBB. Although the ability of PP/SPPs to be transported axonally has been confirmed in rats and monkeys, this has so far been assessed only in the olfactory system. Moreover, the translocation rate is strongly dependent on PP/SPP type and size (Wang et al 2007, 2016).

**d. Direct delivery into the heart**

Although delivery of PP/SPPs or PP/SPP-labeled cells to the heart has in most studies been by intravenous injection, more direct delivery to the myocardium can be

achieved in several ways. This has the advantage of bypassing the general circulatory system, which invariably leads to unintended entrapment of PP/SPPs and PP/SPP-labeled cells in other tissues, especially the lungs. Several types of PP/SPPs have been injected intramyocardially in animal models (reviewed in Suarez et al 2015). In human subjects, autologous progenitor cells (in most cases unlabeled) have been delivered by means of a) arterial and venous catheters into the coronary vessels feeding the infarcted and ischemic tissue, b) transendocardial injections, c) guided electromechanical mapping directly into infarcted myocardium, or d) direct epicardial injections (reviewed in Chen et al 2017; Terrovitis et al 2010), and these approaches can all be used for PP/SPP-labeled cells.

**C. Limitations**

Stem cell labeling and tracking is subject to several limitations, especially in the context of long-term imaging. In addition to PP/SPP degradation and potential toxicity (discussed below), loss of signal can occur through dilution of PP/SPPs by cell division (Zhu et al. 2006). Stem and progenitor cells may continue to proliferate after transplantation, and this will dilute the PP/SPPs in daughter cells, with subsequent loss of signal, potentially limiting the time window for observation to as little as a few days, although Küstermann and colleagues have shown that many cycles of proliferation are needed to decrease the contrast below cell detectability (Küstermann et al., 2008). On the other hand, an advantage of PP/SPP degradation or clearance is that this limits biological impact, avoiding long-term effects that may be difficult to define in clinical trials. For this reason, some PP/SPPs, such as MPIOs, have been intentionally designed to be biodegradable (Nkansah et al 2011, Shapiro 2015).

It is also difficult to quantify the number of PP/SPP-labeled cells *in vivo* because the contrast-generating susceptibility effect is not linear, neither in resultant contrast nor in affected volume. Thus, the MRI signal represents the overall concentration of PP/SPPs in a certain volume, which may not translate easily into cell number, although if labeled cells are well enough distributed cell counting is possible (Afridi et al 2017). MRI signal may also be confused with certain endogenous conditions,

such as accumulations of hemosiderin following hemorrhage, frequently seen at the site of myocardial infarction (van den Bos et al. 2006). Detection of PP/SPPs *in vivo* also does not distinguish among live and dead PP/SPP-labeled cells and PP/SPPs secreted or exocytosed by labeled cells. Dead cells containing PP/SPPs and secreted or exocytosed PP/SPPs can moreover be taken up by neighboring cells or phagocytized by macrophages or microglia, and be carried off on entirely misleading routes of migration thereafter (Amsalem et al. 2007; Ramos-Gómez et al. 2015).

**D. Imaging platforms**

**1. MRI**

PP/SPPs produce their labeling effect by disturbing the homogeneity of the static magnetic field $B_0$ of the MRI system. MRI signal intensity and contrast are mainly defined by the proton density $\rho$ and relaxation times T1 and T2, characteristic for the investigated tissue. Additionally, the relaxation time T2* takes magnetic field inhomogeneities into account, as are caused e.g. by paramagnetic impurities:

$$1/T2^* = 1/T2 + \gamma\Delta B$$

Where $\gamma$ is a constant and $\Delta B$ reflects the deviation from the static magnetic field $B_0$. In consequence, a massive magnetic field disturbance by iron oxide nanoparticles will result in extremely short T2* relaxation, letting the signal decay rapidly and resulting in signal loss. Low signal intensity of tissue or cells labeled with iron oxide nanoparticles then produces strong negative contrast to the non-labeled adjacent tissue:

$$C=(S_{labeled} - S_{nonlabeled})/S_{nonlabeled}$$

To keep the signal of the surrounding tissue ($S_{nonlabeled}$) high, only moderate T2*-weighting of the images is preferred while strong labeling (i.e. high $\Delta B$) will reduce T2* to the point of total signal loss.

Alternatively, T1-weighting can be used in cases of weak label effect. PP/SPPs also reduce T1 in labeled cells, thus generating a hyperintense signal in T1-weighted images and resulting in positive contrast to the adjacent tissue. It should be noted,

however, that this positive T1-dependent contrast works only for low label concentrations when the influence on T2* is not too strong. Otherwise, the T2* signal decay is too prevailing and T1-weighted signal is no longer detectable.

Due to the application limit of T1-based positive contrast, the negative contrast of T2* sensitivity is the most widely used detection method. The effect of T2* bleeding into adjacent regions will spatially enhance the apparent size of signal loss, making detectability easier but also overestimating the spot size of the labeled cells.

The fact that high label concentration drives the T2* to too short values means that the signal is completely erased. Therefore, stronger magnetic fields are no longer important to generate high (negative) contrast. However, higher demands on spatial resolution of small clusters of labeled cells require high Boltzmann factor for strong enough signal in decreasing voxel sizes. Thus, through the need for detecting and resolving very small cell clusters, the voxel resolution must be high. Otherwise, partial volume effects dilute the contrast effect of the iron oxide label. Thus, spatial resolution of 70-150 μm isotropic is desirable. For such resolution, MRI systems operating at 7T or higher magnetic fields are preferable. Otherwise, restricted S/N must be compensated by longer times for signal averaging, which, however, quickly produces a conflict with the demands of keeping the physiological conditions of the animal or patient stable in *in vivo* experiments.

In summary, for MRI of PP/SPP-labeled cells, high field T2*-weighted pulse sequences are recommended with long repetition time (TR) values to avoid counter-effective T1 influence. Optimal sensitivity requires high spatial resolution to minimize T2* bleeding and contrast dilution through partial volume effects. Depending on the PP/SPP used, resolution can be great enough to detect single labeled cells (Figure 2). It is noteworthy that although the T2*-sensitive approach is most sensitive, it typically allows only qualitative analysis without permitting quantification of label amount (or cell number, unless a small enough number of labeled cells are well distributed, see for example Afridi et al 2017).

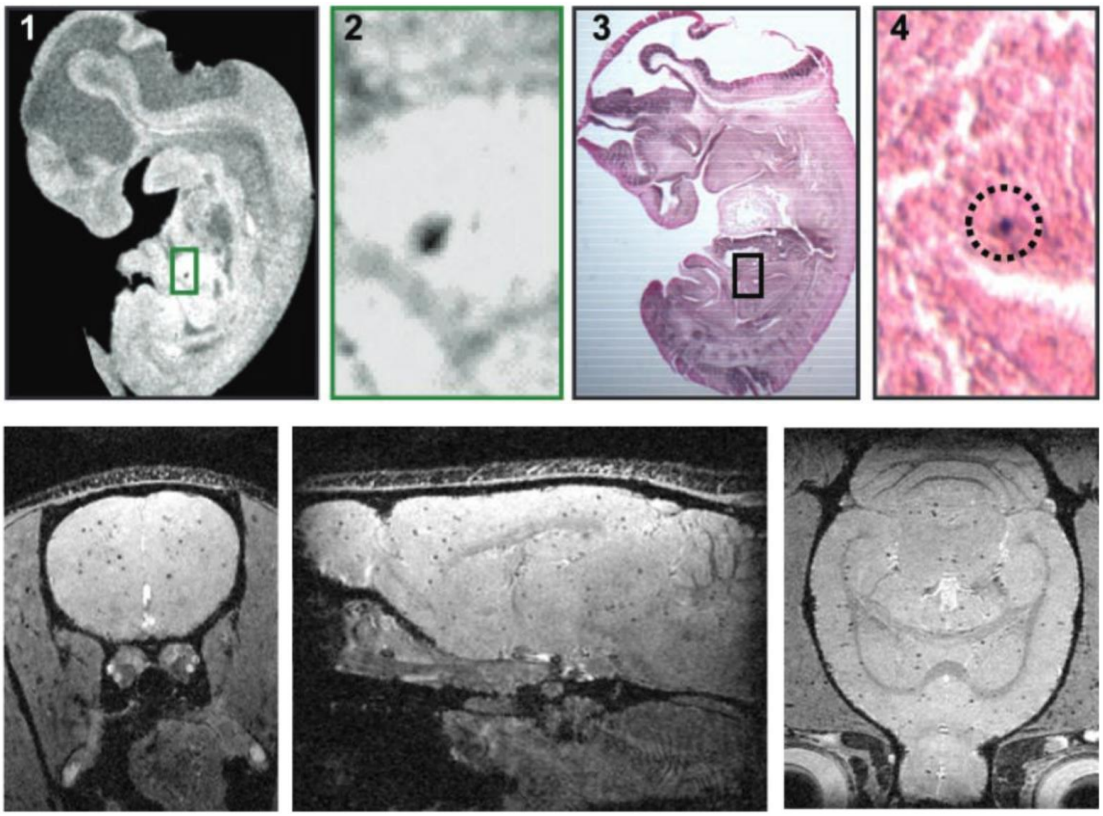


*Figure 2. Upper panel: Comparison of T2*-weighted 3D MRI detection and postmortem Prussian Blue histological staining of a mesenchymal stem cell labeled with a single MPIO in an E13 mouse embryo (from Shapiro et al 2004). Lower panel: Example of T2*-weighted MRI signals associated with MPIO-labeled MSCs in mouse brain, in a study utilizing convolutional neural network (CNN)-based automated counting of MPIO-labeled cells. From Afridi et al (2017), with permission.*

**2. Synchrotron radiation X-ray computed microtomography (micro-CT)**

One of the limiting factors in the interpretation of *in vivo* cell tracking is 3D-resolution. In this regard, μCT offers high sensitivity and thus increased spatial resolution, reaching as low as a few μm. Although paramagnetic iron oxide particles are less suited than gold particles to generate sensitive CT contrast in labeled cells (Hainfeld et al., 2006), excellent results have been obtained with impressive detectability of iron oxide-labeled cells in rodent muscle tissue (Farini et al., 2012; Torrente et al., 2006).

A significant development in μCT imaging is the use of synchrotron radiation as an X-ray source (Albers et al., 2018; Kinney and Nichols, 1992). Here, the high flux of photons allows the resolution of subtle variations in absorptivity and therefore internal structure. Imaging by synchrotron X-ray sources, however, is limited to small

specimens, typically 5–10 mm in diameter. The spatial image resolution is down to a few μm, but new "nanotomographic" devices are available, with resolution down to a few hundred nm (Withers, 2007).

In addition to the absorption mode of synchrotron radiation imaging, a phase-contrast mode can be chosen that is particularly sensitive with respect to discriminating interfaces and edges between two different adjacent materials or tissue types (Marinescu et al., 2013). By combining these two modes of action, impressive structural details have been reported in mouse tissues, with the use of iron oxide nanoparticles as a CT contrast agent (Torrente et al 2006) (Marinescu et al., 2013) (Figure 3).

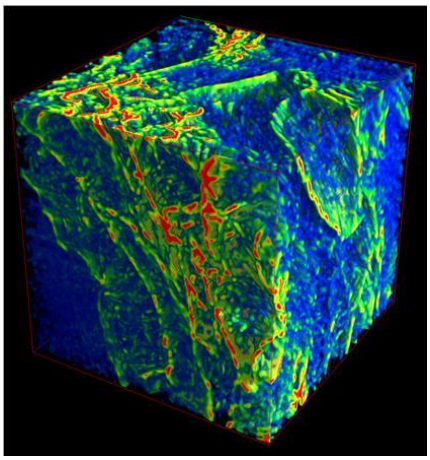

*Figure 3. Ex-vivo 3D visualization of the distribution of PP/SPP-labeled CD133+ stem cells (red), migrating from blood vessels (green) into surrounding muscle tissue (blue), 24 h after intra-arterial injection into dystrophic mouse. From Torrente et al (2006), with permission.*

**E. Adjunct tracer modalities**

Several auxiliary imaging modalities can be combined with PP/SPPs, providing favorable adjuncts for later histological inspection of biopsy or autopsy material. Some of these can be intrinsic to the PP/SPPs themselves, such as histological methods for detecting the iron in PP/SPPs or incorporation or conjugation of PP/SPPs with fluorophores or other visualizable molecules. Others can provide a separate, "parallel" label. Each has its own caveats, advantages and disadvantages. Many are also problematic in a clinical setting, and their use may therefore be restricted to animal or *in vitro* experiments.

**1. Direct detection of PP/SPPs**

**a. Prussian Blue-mediated detection of iron**

Prussian Blue is a histological dye that has been used for many years to reveal the iron content of cells and tissues. It involves the application of a mixture of potassium ferricyanide and acid to histological sections. Upon encountering concentrations of Fe3+ in the section, the ferricyanide forms insoluble deposits according to the reaction:

$$4Fe^{3+} + 3[Fe^{II}(CN)_6]^{4-} \rightarrow Fe^{III}[Fe^{III}Fe^{II}(CN)_6]_3$$

Many studies employing PP/SPPs for *in vivo* imaging have used Prussian Blue staining in biopsy material or post mortem as a means to corroborate and define the location of PP/SPP-labeling. The results, however, can be confounded by high endogenous iron content. An alternative that has been tested is to dope iron oxide PP/SPPs with europium and use laser ablation combined with inductively coupled plasma mass spectrometry (LA-ICP-MS) to quantitate PP/SPP content in tissue sections (Scharlach et al 2016).

**b. Fluorophore-conjugated PP/SPPs**

Some PP/SPPs, particularly MPIOs, have been conjugated with a variety of fluorophores to permit combined MRI and whole animal fluorescence imaging *in vivo* (see for example Sumner et al 2010, Boulland et al 2012).

**c. Non-fluorescently conjugated PP/SPPs**

PP/SPPs can also be conjugated with non-fluorescent molecules, which cannot be visualized *in vivo* but can be used to pinpoint the location of PP/SPPs post mortem or in biopsy material (Shen TT et al 1996, de Palma et al 2007, Amstad et al 2009, Wei et al 2012). Certain enzymes (such as horseradish peroxidase and alkaline phosphatase) can be used with colorigenic substrates. Antibodies and biotin can be revealed immunohistochemically or by binding of streptavidin. Avidin can also be conjugated directly to PP/SPPs (Yang et al 2015).

**2. Parallel methods for cell labeling**

**a. Lipophilic fluorescent probes**

**CellTracker CM-DiI (Invitrogen, C-7001)** is an octadecyl indocarbocyanine (DiI) derivative that is somewhat more water-soluble than DiI, thus facilitating the preparation of staining solutions for cell suspensions. CellTracker CM-DiI contains a thiol-reactive chloromethyl moiety (CM) that allows the dye to covalently bind to cellular thiols. Thus, unlike other membrane stains, this label is well retained in the cells throughout several mitotic divisions, and there is limited intercellular dye diffusion (1, 2). Positive features include good delineation of cell morphology, membrane delimitation and stable fluorescence. Photoconversion for electron microscopic visualization is also possible. Negative features include a tendency to redistribute within the cell due to membrane dynamics (for example internalization), and not being tissue-fixable. Combination with PP/SPPs has been reported by Odintsov et al 2013 and Marikides et al 2013.

**b. Nucleic acid-specific and organelle-specific fluorescent probes**

A number of dyes and probes exist for labeling nucleic acids and certain organelles relatively selectively, and some of these have been used to label living cells *in vitro* and *in vivo*. Hoechst dyes, TOPRO and TOTO-3 are commonly used to label DNA (Martin et al 2005), but they can also label RNA and are thus not exquisitely specific for DNA. Oft-used organelle-specific tracers include MitoTracker probes for mitochondria and LysoTracker probes for lysosomes.

**c. Fluorescently and non-fluorescently conjugated dextrans**

Conjugated dextrans provide an innate, cytoplasmic label that is stable and non-toxic, and that can be visualized both fluorescently and non-fluorescently. They can be delivered in a variety of ways, including through intracellular injection, electrofection, lipofection and endocytosis. Dextrans can also be conjugated with activity-dependent probes, for example to permit visualization of intracellular Ca++ dynamics, and can be used to carry drug payloads (Glover 1995, 2014). Positive features include limited degradation, stability over weeks *in vivo*, even distribution throughout the cytoplasm, and they are tissue-fixable and superbly compatible with immunohistochemistry and streptavidin-biotin-mediated visualization procedures

for light and electron microscopy. Negative features include the need to be internalized efficiently, limited diffusion over long distances (for example in very long axons), and dilution with cell division. Many types of PP/SPPs are dextran-coated and can thus be coupled to these same approaches directly (see Sections E.1.b and E.1.c.).

**d) Qdot® nanocrystals** are fluorophores that absorb light and re-emit photons at a different wavelength, but the mechanism of fluorescence is quite different compared to traditional fluorophores. Rather than $\pi \rightarrow \pi*$ electronic transitions based on excitation wavelength, it is the size of the nanocrystal that determines the color emission. Qdot nanocrystals are nanometer-scale (roughly protein-sized) atom clusters, containing from a few hundred to a few thousand atoms of a semiconductor material (cadmium mixed with selenium or tellurium), which is coated with an additional semiconductor shell (zinc sulphide) to improve the optical properties. Positive features include exceptionally high and stable fluorescence and the feasibility of visualizing multiple fluorescent labels with the same excitation wavelength. Negative features include dilution with cell division and not being tissue-fixable and thus having a tendency to be lost during histochemical processing. Examples of Qdot labeling in connection with cell implantation experiments can be found in (Giulani et al 2011, Rossini et al 2011.

**e) Genetically encoded fluorescent proteins**

Cells can be genetically modified through gene editing or transduced *in vitro* by incubation with lentiviral or other vectors to enable the expression of a spectrum of fluorescent proteins (Tennstaedt et al. Biomaterials 44, 143-1154, 2015). Positive features include highly stable expression that can be targeted to specific subcellular domains, no dilution with cell division, being tissue-fixable, and the option of amplifying (or changing) the fluorescent signal using immunohistochemistry or other amplification systems. Fluorescent proteins can also be engineered for use in functional assessment (Ca++, voltage-sensitive, FRET, CRET imaging), or cellular manipulation (optogenetics). Negative features include the difficulty of achieving 100% transduction efficiency, potential cell type- or state-specific expression, and

the possibility that overexpression may influence cell behavior. Studies exemplifying the combined use of PP/SPPs and fluorescent proteins include (Rossini et al (2011), Boulland et al (2012), Rai et al (2013) and Savi et al (2016).

## III. Molecular and cellular interactions and effects of PP/SPPs

### A. Protein corona

Following *in vivo* administration, PP/SPPs are exposed to blood or other physiological fluids containing ions, proteins, sugars and other small molecules. Based on the surface charge and other physicochemical properties of the PP/SPPs, these molecules adhere to the PP/SPP surface and form a bio-corona, also referred to as the "protein corona" (Treuel et al 2015), which not only constitutes the outermost surface through which cells thereafter recognize and interact with PP/SPPs, but also can change or modify key PP/SPP properties, including size, surface charge, stability and magnetic properties (Safi et al 2011, Pavlin & Bregar 2012, Tenzer et al 2013). Interaction with PP/SPPs can also alter the tertiary structure of proteins within the protein corona, exposing otherwise hidden epitopes and influencing the immune response to the PP/SPPs (Lundqvist et al 2008, Deng et al 2011). The protein corona can also assimilate immunologically active proteins, such as antibodies, opsonins and complement proteins, which mediate immune cell responses (Chen et al. 2016). PP/SPPs that are recognized by macrophages are quickly internalized and removed from the circulation, thus limiting their ability to reach tissue targets.

### B. Internalization and intracellular trafficking

PP/SPPs are most frequently internalized through one of the energy dependent endocytic pathways, such as phagocytosis, micropinocytosis, clathrin- or caveolin-dependent pathways and several others (Iversen et al 2011). The pathway utilized depends on the cell type (Kuhn et al 2014, Lojk et al 2015), the physicochemical properties of the PP/SPPs (Akinc and Battaglia 2013), and the composition of the protein corona (Safi et al 2011). Due to the inherent complexity of uptake systems and variability among PP/SPPs, the internalization pathway and rate of internalization have to be determined empirically for each PP/SPP type. Generally, charged PP/SPPs are more readily internalized due to protein corona formation and

electrostatic binding of PP/SPPs to the cell membrane. Recognition and uptake of PP/SPPs can also be mediated through cell membrane receptors that recognize specific proteins in the protein corona.

Several examples have been described in which the specific mechanism of uptake has been determined. 20-60 nm carboxydextran-coated iron oxide PP/SPPs have been shown to enter macrophages via scavenger receptor A-dependent clathrin-mediated endocytosis (Raynal et al. 2004; Lunov et al. 2011). Clathrin-mediated endocytosis is also involved in the internalization of poly(vinylalcohol/vinylamine)-coated iron oxide PP/SPPs into human melanoma cells (Cengelli et al. 2010), poly(4-vinylpyridine), of PEG-coated maghemite PP/SPPs into primary rat aortic vascular smooth muscle cells (Ali et al. 2015), of dimercaptosuccinate-coated iron oxide PP/SPPs into oligodendrocytes (Petters et al. 2014) and primary rat cerebellar neurons (Petters and Dringen 2015), and of dextran-coated PP/SPPs into various mammalian cell lines (Soenen et al. 2009). Polyacrylic-acid coated PP/SPPs have been shown to be taken up through macropinocytosis and clathrin-dependent endocytosis in several mammalian cell types (Bregar et al. 2013; Lojk et al. 2015). Amino-functionalized PP/SPPs and carboxyl-functionalized PP/SPPs have been shown to be taken up by phagocytosis and micropinocytosis, respectively, in human prostate-cancer PC-3 cells and transformed human breast epithelial cells (Kralj et al. 2012), and carboxymethyl dextran-coated iron oxide PP/SPPs have been shown to be internalized by macropinocytosis in CaCo-2 human colon cancer cells (Ayala et al. 2013).

Targeting to specific cells/tissues can be improved by functionalizing PP/SPPs with ligands or antibodies that bind to receptors specific for the desired endocytic pathway (Masserini 2013). Such ligands include manose-6-phosphate, transferrin and nicotinic acid to target receptors to clathrin-coated vesicles (Bareford and Swaan 2007) and antibodies, components of the complement system and bacterial components to induce phagocytosis (Freeman and Grinstein 2014). Antibodies or ligands can also be used to target cell-type specific membrane proteins, such as those expressed primarily on cancer cells or typical of inflammation sites. For

example, coating PP/SPPs with dextran sulfate, a ligand of the macrophage scavenger receptor A, has been shown to improve their targeting of macrophage-infiltrated atherosclerotic lesions in an *in vivo* mouse model (Tu et al. 2011). MPIOs conjugated with monoclonal antibodies against VCAM-1 and P-selectin have been successfully targeted to inflamed vasculature in a mouse model of atherosclerosis (McAteer et al. 2008).

Conversely, the physicochemical properties of PP/SPPs and their coating can also be utilized and optimized to avoid cellular recognition. PEG is a frequently used coating that significantly reduces opsonization, decreases recognition by immune cells and thus prolongs the circulation time of PP/SPPs *in vivo* and increases their chances of reaching the target tissue (Liu et al. 2011; Ni et al. 2012). PEG has been FDA approved and used in several PP/SPP formulations (Bobo et al. 2016). Certain PEGylated formulations have recently been shown to have immunogenic properties, however, exemplified by activation of the complement system through classical and alternative pathways by PEGylated liposomes and PEGylated multi-walled carbon nanotubes *in vivo* in pigs and *in vitro* in human serum (Szebeni et al. 2006; Moghimi et al. 2010; Andersen et al. 2013). Strong activation of the complement system by dextran-coated and oleic acid-coated PP/SPPs has also been observed (Banda et al. 2014; Wang et al. 2016; Wolf-Grosse et al. 2017)

Once internalized, PP/SPPs undergo intracellular trafficking and processing, which strongly depends on the internalization pathway and the cell type. A typical result is lysosomal accumulation. Endolysosomal trafficking has been demonstrated or presumed for PLGA- (Zhang et al. 2016), poly(vinylalcohol/vinylamine)- (Cengelli et al. 2010), citrate-, dextran- (Wu et al. 2010), folic acid- (Kumar et al. 2012) and dimercaptosuccinate-coated PP/SPPs (Geppert et al. 2011). After being sequestered in acidic lysosomes PP/SPPs often tend to accumulate in neutral pH storage vesicles in the perinuclear region (Bregar et al. 2013; Lojk et al. 2015; NDong et al. 2015).

**C. Degradation, iron release and metabolism**

Most PP/SPPs are degraded slowly despite the exposure to the acidic lysosomal environment. Gradual degradation of PP/SPPs has been reported to take from a few days to a few weeks depending on PP/SPP size, the pH to which they are exposed and their surface coating, which is the first layer exposed to the degradative lysosomal environment (Arbab et al. 2005a; Lévy et al. 2010; Soenen et al. 2010a; Malvindi et al. 2014). Degradation of the coating layer exposes the iron oxide core to the acidic lysosomal environment, leading to etching and the release of free metal ions (Sabella et al. 2014). This leads to a gradual decrease in the paramagnetic core diameter and thus a gradual loss of imageable labeling (Gutiérrez et al. 2015; Volatron et al. 2017). Despite this pitfall, degradation is necessary for clearance of PP/SPPs from the organism once they no longer are needed for tracking. Biodegradable micron-sized PP/SPPs have been developed specifically to enhance this clearance (Shapiro 2015).

The iron ions released from PP/SPPs are subjected to intrinsic cellular metabolism, which principally involves transferrin-mediated uptake. The acidic environment in late endosomes and lysosomes releases Fe3+ ions from internalized transferrin and a ferrireductase enzyme (divalent metal transporter 1; DMT-1) reduces Fe3+ to Fe2+, allowing its transport across the endosomal membrane to the cytoplasm. In the cytosol, Fe2+ is either used immediately or stored as ferritin, which can sequester larger amounts of iron in its chemically less reactive ferrihydrite form and thus also achieves detoxification in the case of iron overload. The daily iron requirement of an adult person is 20-25 mg, most of which is used for the daily production of new erythrocytes. In a healthy person, only 1-2 mg of iron is obtained through food, while the rest is recycled from old and damaged erythrocytes, which are broken down by macrophages (Hentze et al. 2004). Radiolabelled iron derived from PP/SPPs has been detected in hemoglobin in intracellular iron storages one week after PP/SPP injection, confirming a relatively rapid onset of intracellular degradation and channeling of PP/SPP-derived iron into the iron pool of the organism (Weissleder et al. 1989; Pouliquen et al. 1991).

Entry of PP/SPP-derived iron into cellular metabolic pathways has also been demonstrated *in vitro*. Dimercaptosuccinic acid (DMSA)-coated PP/SPPs with a core diameter of about 10 nm caused a concentration- and time-dependent increase in cell iron content and storage and ferritin accumulation in cultured astrocytes (Geppert et al. 2012). Similarly, commercially available PP/SPPs (VSOPs, Endorem, MLs and Resovist) increased cellular transferrin levels after 24 h incubation, but the levels returned to normal after an additional 6 days of culture without PP/SPPs (Soenen et al. 2011).

**D. Excretion**

Another possible PP/SPP fate is excretion back into the extracellular space. The mechanisms of PP/SPP excretion are not well understood, but it is believed that some vesicles containing PP/SPPs can undergo exocytosis as a result of either normal membrane recycling or membrane repair during cellular stress (Sakhtianchi et al. 2013). PP/SPPs can also be exocytosed after passing through epithelial cells in the process of transcytosis, which is typical for caveolin-dependent uptake (Parton and del Pozo 2013; Kafshgari et al. 2015). In this case, the cargo normally bypasses lysosomes and is secreted intact on the other side of the cell. This route could be employed for delivery across endothelial barriers to underlying target tissues (Wang et al. 2011; Wang 2014). In most other cases, exocytosis is not desirable, since it removes PP/SPPs from the cells, eliminating labeling. Moreover, exocytosed PP/SPPs are available for internalization by other cell types like macrophages, thus reducing the cell-type specificity of labelling and tracking.

**E. Biocompatibility and toxicity**

One of the most important requirements for a rational use of PP/SPPs in cell labeling and tracking is biocompatibility. Most PP/SPPs have been designed with this in mind, and few studies report any severe or long-term toxic effects (Arbab et al. 2003a, 2004). Indeed, degradation and the concomitant slow release of iron ions has been proposed as a treatment for iron deficiency anemia in adult patients with chronic kidney disease, exemplified by FDA-approved Furoximol nanoparticles (Landry et al. 2005). However, the prolonged presence of PP/SPPs in cells can have negative

consequences. Although the amount of PP/SPP-derived iron oxide injected or implanted (0.5-0.8 mg/kg in the case of MRI contrast agents) generally does not exceed daily dietary iron requirements and the release is gradual, increasing evidence indicates that free Fe ions released through degradation may induce cellular stress locally (Sabella et al. 2014; Wu et al. 2014). Increase of iron content can be enough to potentially induce the formation of reactive oxygen species (ROS; Hohnholt and Dringen 2011; Wu et al. 2014), apoptosis, inflammation (Lunov et al. 2010b) and increased ferritin expression as an adaptive response to counteract the increase in iron concentration (Laskar et al. 2012). Prolonged intracellular PP/SPP presence has been suggested to induce autophagy, lysosomal dysfunction and defects in intracellular trafficking, cell signaling and vesicle fusion, all of which are important for cellular homeostasis, removal of damaged cellular components and stress responses (Stern et al. 2012).

Some negative effects on cellular differentiation and function have been reported, and these are likely to be related both to the type of PP/SPP used and the cell type. PP/SPPs have been reported to inhibit osteogenic differentiation in human mesenchymal stem cells (Chen et al. 2010), reduce neurite outgrowth by PC12 cells (Soenen et al. 2010a), and reduce antioxidant defenses and increase oxidative stress in models of neurodegenerative diseases (Munoz et al 2016) (Núñez et al. 2012). Autophagy has been shown to be induced by PP/SPPs in lung epithelial cancer cells (Yokoyama et al. 2011; Khan et al. 2012), HeLa cells (Huang et al. 2015) and breast cancer cells (Zhang et al. 2016). Certain PP/SPPs can also damage lysosomes through the process of lysosomal escape (“proton-sponge-effect”) and induce release of the lysosomal enzyme cathepsin D (Cengelli et al. 2010), which acts as a signal for apoptosis (Serrano-Puebla and Boya 2016). Moreover, PP/SPPs have been reported to non-specifically associate and damage other organelles in the cell, such as mitochondria, leading to mitochondrial mediated induction of apoptosis (Parhamifar et al. 2010; Park et al. 2014; Zhang et al. 2016). PP/SPPs have also been reported to diminish cell proliferation and the efficiency of protein expression, and to affect the cell cytoskeleton by sterically hindering the formation of actin fibers, which could affect cell migration and differentiation (Soenen et al. 2010b, 2011; Diana et al.

2013). One study also reported a PP/SPP-induced long-lasting membrane depolarization in neural stem cells and a hyperpolarization of their mitochondrial membranes (Pongrac et al. 2016).

One of the most frequently observed mechanisms of PP/SPP toxicity is the formation of ROS and the induction of oxidative stress. ROS formation can either result from PP/SPP-induced cell stress and damage or from the iron-catalyzed Fenton reaction, which can occur on the surface of PP/SPPs or be catalyzed by released iron ions (Kehrer 2000; Wu et al. 2014). The contribution of iron to ROS induction has been confirmed through the use of iron chelators (Soenen et al. 2011, Aguirre et al 2015). Increase in ROS formation has been observed for several types of PP/SPPs, including several that are commercially available (VSOPs, Endorem, Resovist; Soenen et al. 2011). Carboxydextran-coated PP/SPPs accumulated by macrophages *in vitro* did not affect cell viability 24 h after labeling, but induced the formation of ROS, caspase 3-dependent apoptosis, and secretion of tumor necrosis factor α (TNFα) 2 days later (Lunov et al. 2010a, Lunov et al. 2011). PP/SPPs have been reported to induce the formation of ROS and to cause membrane damage, cell cycle arrest and apoptosis and to reduce viability in PC12 cells *in vitro* and to cause oxidative damage in the brain *in vivo* (Wu et al. 2011). Dimercaptosuccinate (DMSA)-coated PP/SPPs have been reported to cause an increase in ROS in oligodendrocytes (Hohnholt and Dringen 2011) and astrocytes (Geppert et al. 2012). Interestingly, astrocytes show a high resistance to PP/SPP-induced oxidative stress compared to other cell types, likely related to their intrinsic role as regulators of metal metabolism in the brain (Dringen et al. 2007; Hohnholt and Dringen 2013)

ROS formation is especially problematic in brain tissue due to its high oxygen consumption (20% of the total oxygen consumption of the organism), high lipid content (particularly polyunsaturated fatty acids, which contain double bonds and are thus vulnerable to free radical attacks and lipid peroxidation), weak antioxidant defenses and high intrinsic iron content. Moreover, chronic ROS formation and inflammation have been shown to be associated with the progression of neurodegenerative diseases and it is not yet clear if ROS is caused by the disease or

vice versa (Urrutia et al 2009, Urrutia et al 2014, Munoz et al 2016). Iron depositions are commonly observed in neurodegenerative disorders such as Alzheimer's and Parkinson's (Liu et al. 2010; Mochizuki and Yasuda 2012; Ayton and Lei 2014). A positive feedback loop between iron accumulation, oxidative stress and neurodegeneration-linked protein accumulations has been suggested that PP/SPP-derived iron might aggravate further (Yarjanli et al. 2017) (Urrutia et al 2014).

## IV. Preclinical and clinical applications in the context of cardiac disease

### A. Background

Advanced heart failure (AHF) is the leading cause of death worldwide, and despite unquestionable progress in prevention and treatment over the last 25 years, its incidence continues to rise. According to recently published statistics, 6.4 million patients suffer from AHF in the USA with 960,000 new cases per year (Circ AHA statistics). AHF can be considered a world epidemic because similar progressive incidence has been reported in Europe and Asia. AHF may reflect a progression of underlying myocardial disease and/or result from dysfunction of compensatory mechanisms without any changes in workload on the heart. AHF incidence has increased because the use of revascularization, fibrinolytic therapy and anti-arrhythmic drugs allows survival of patients with large infarcts. At the final stage, heart transplantation remains the treatment of choice. Nevertheless, a critical shortage of donor organs makes it imperative to restrict transplantation to the most disabled patients, who are likely to derive the maximum benefit. Unloading the heart by cardiac assist devices, restoring ventricular anatomy by myocardial left ventricular resection, or removing the detrimental impact of persistent overload all attenuate the evolution of the disease. However, the clinical limitations of all of these approaches indicate a poor understanding of the basic mechanisms of AHF and justify the search for new therapeutic options.

Regenerative medicine opens a new therapeutic avenue with the potential to change the natural history of heart failure. The recent introduction of stem cells into the arena of cardiology provides new tools for understanding regenerative mechanisms in the normal and pathological heart. Experimental (15-18) and clinical

(5-14) studies have been undertaken in an attempt to treat degenerative heart disease by implantation of exogenous stem or progenitor cells. Although controversies still exist on the interpretation of the clinical observations (Eschenhagen et al 2011), studies on stem cell-based therapies have shown promising results for treatment of myocardial infarction (reviewed in Gyöngyösi et al 2018), peripheral artery occlusive disease (Tateishi-Yuyama et al 2002, Higashi et al 2004, Huang et al 2004) and congenital heart diseases (Sitaram et al 2018). However, this approach has some limitations with respect to efficiency and the considerable time required to regenerate damaged heart tissue. Stimulation of resident stem cells may provide a more feasible approach for implementing cardiac tissue regeneration. Cell tracking in connection with the implantation of cardiac stem or progenitor cells, or of differentiated cardiomyocytes, or of mesenchymal stem cells with modulatory effects on inflammation and stimulatory effects on resident stem cells, is a key element in the development of such therapies.

A reproducible and efficient cell tracking system for human cardioregenerative studies has not yet been identified, however. This issue needs to be resolved because lack of knowledge about the short and long term fates of implanted cells strongly limits evaluation of the clinical benefit and thus the development of cell-based regenerative approaches. An additional consideration is the risk of ionizing radiation associated with radiology-based cardiac imaging, particularly when serial analyses are required (Gerber et al 2009, Luo et al 2017). Implementing non-radioactive imaging procedures, particularly those based on MRI, is therefore important.

**B. Preclinical studies**

A number of preclinical studies have supported the idea of using PP/SPP-labeling as a means of tracking cells that may contribute to cardiac regeneration. Engraftment of ESCs, MSCs or skeletal muscle–derived myogenic precursor cells and their distribution in cardiac tissue has been confirmed in rodent and swine models of myocardial infarction (Himes et al. 2004; Arai et al. 2006; Mani et al. 2008). Feridex-labeled mouse ESCs injected post infarction in a mouse myocardial infarction model

followed by MRI tracking showed a significant restoration of the injured myocardium (Arai et al. 2006). Similarly, Feridex-labeled swine MSCs successfully engrafted in an infarction lesion (Kraitchman et al. 2003), reduced scar formation and contributed to substantial normalization of cardiac function (Amado et al. 2005). On the other hand, detected label has been misleading in some studies. In one such study, SPION-labeled MSCs were injected into the infarction site in a rat model of myocardial infarction. The cells remained at the site of infarction and a strong MRI signal could be detected up to 3-4 weeks after administration. However, histological and genetic analyses revealed that most of the PP/SPPs by this time were located in myocardial macrophages at the infarction site, suggesting that the majority of SPION-labeled MSCs had died and been phagocytosed (Amsalem et al. 2007; Terrovitis et al. 2008).

**C. Clinical studies**

The aim of cardiac cellular transplantation is to repopulate the healing myocardium with cells that could restore contractility and blood supply. In human subjects, autologous progenitor cells have been delivered by means of a) arterial and venous catheters into the coronary vessels feeding the infarcted and ischemic tissue, b) transendocardial injections, c) guided electromechanical mapping directly into infarcted myocardium, or d) direct epicardial injections (Dib et al 2010, Sharif et al 2011). In several studies there was improved blood flow and left ventricular function, suggesting that introduction of autologous progenitor cells appears to be feasible and safe and might confer short-term therapeutic benefit (reviewed in Gyöngyösi et al 2018). Nevertheless, there is substantial variability in the factors and conditions involved in validating the benefits of such cellular therapy. A number of questions regarding the cell type to be used and the methods of cell harvesting, implantation and cell tracking remain incompletely answered (Frangioni et al 2004, Fu et al 2010, Nguyen et al 2014)

Several studies have documented the results of clinical trials aimed at tracking exogenous cells in the heart of normal volunteers (Richards et al 2012) or assessing the cellular processes involved in tissue repair following myocardial infarction (Florian et al 2014, Alam et al 2017). According to the NIH *ClinicalTrials.gov* database, only one clinical trial (NCT03651791) utilizing USPIO-labelled MSCs in the

ischemic heart has been completed recently, with as yet unpublished results. Experimental approaches using theranostic nanoparticles carrying bioactive molecules including a number of specific growth factors have also been combined with cardiac imaging of regenerative processes showing encouraging results (Chen J et al 2017, Guo et al 2012, reviewed in Zhu et al 2016, Bengel et al 2017, Radomska et al 2016).

## V. Preclinical and clinical applications in the context of neurological disease

### A. Background

The transplantation of stem cells into the injured brain is considered a promising approach for many neurological disorders such as Parkinson's disease, stroke and multiple sclerosis, as it may provide clinical benefits through neuronal replacement, remyelination and neuroprotection (Lindvall and Kokaia, 2006). When stem cells are transplanted into injured brain tissue, which constitutes a potentially hostile environment of limited oxygen and nutrient delivery and inflammation, it is essential to monitor the fate and migration of the implanted cells to correctly interpret potential beneficial effects. Non-invasive *in vivo* cell tracking is therefore a key element in the development and clinical translation of novel regenerative therapies. The ideal label in this regard would be nontoxic, retained by target cells over sufficiently long times at easily detectable concentrations, correlate stoichiometrically with cell number and would be cleared rapidly after cell death (Naumova et al., 2014).

### B. Preclinical studies

To meet the above criteria, numerous *in vitro* and animal studies have been performed to develop and optimize loading of neural stem and progenitor cells with PP/SPPs, and to evaluate the effects on cell proliferation and self-renewal, motility, differentiation, transcriptome stability, and signal stability (Neri et al., 2008)(Crabbe et al., 2010) (Boulland et al 2012) (Cromer Berman et al., 2013)(Cianciaruso et al., 2014) (Kallur et al 2011) (von der Haar et al., 2015). These preclinical studies have provided convincing information about the location and migration of stem cell grafts in various animal models of neurological disorders, complementing conventional

histology and behavioral tests in the assessment of recovery. For example, Feridex-labeled neurospheres have been tracked to the site of inflammation in a rodent model of multiple sclerosis (Ben-Hur et al. 2007; Cohen et al. 2010) and have been shown to migrate along an intraparenchymal pathway from the cortical transplantation site in a rodent stroke model (Guzman et al. 2007). SPION-labeled human NPCs have been tracked for one month after transplantation into adult murine brains, and the labeling has been shown not to affect cell viability, proliferation or differentiation capacity (Neri et al. 2008). Focke et al showed that labeling of human NPCs with VSOPs did not affect viability, proliferation or differentiation *in vitro*. Following subsequent transplantation into rat striata, the MRI signal was detected up to three months later (Focke et al. 2008). Boulland et al (2012) demonstrated efficient uptake of MPIOs by NPCs, adult NSCs, and glioblastoma stem cells, with no adverse effects on cell proliferation, migration or differentiation *in vitro*, or on cell migration *in vivo* (Boulland et al 2012). Dil-coated SPIONs have been used to label NPCs to track their migration to glioma tumor sites in rats (Zhang et al. 2004). Endorem-labeled bone marrow stromal cells have been shown to migrate to sites of cortical photochemical lesions in rats, populate the border zone of the damaged tissue during the first week of transplantation, and remain detectable for more than 50 days (Jendelová et al. 2003). Mouse bone marrow MSCs were preloaded with Feraspin XL particles, injected intrathecally, and found to migrate into and persist for up to 14 days in the spinal cord and dorsal root ganglia of ataxic mice (Jones et al 2014).

Since the production of the FDA-approved PP/SPPs Endorem and Resovist was terminated, efficient protocols for labeling stem and progenitor cells with novel PP/SPP formulations have had to be implemented and thoroughly verified (Berman et al., 2011; Frank et al., 2007; Kallur et al., 2011). Several groups have synthesized and characterized novel PP/SPPs that are suitable for neural stem and progenitor cell labeling. Jirakova et al. designed poly-l-Lysine SPIOs and labeled human induced pluripotent stem cell-derived neural precursor cells (iPSC-NPs) without affecting cell proliferation or neuronal differentiation (Jirakova et al., 2016). Lu et al. developed novel cationic polymeric micelles based on the amphipathic polymer of

biodegradable hydrophilic poly(aspartic acid-dimethylethanediamine) that were conjugated with two molecules of hydrophobic cholic acid by lysine (Lu et al., 2017). SPIOs and fluorescent Nile Red were simultaneously loaded into the micelles. These multifunctional particles were used to label immortalized neural stem cells (NSCs) without detrimental effect and enabled *in vivo* detection of $5x10^5$ pre-labeled cells in the rat brain. Aswendt et al. designed fluorescent derivatives of the commercially available aminodextran-containing magnetite FeraTrack Direct FTD particles (Miltenyi Biotec, Germany), which did not require transfection agents to efficiently label human and mouse NSCs (Aswendt et al., 2015). These particles had no effect on proliferation, migration and differentiation capacity *in vitro* and were used to track $1.5x10^5$ transplanted, pre-labeled NSCs in the mouse brain longitudinally by MRI *in vivo*. To monitor the viability of the cells directly, a luciferase was also expressed in the NSCs for bioluminescence imaging (BLI), which correlated directly with the number of viable cells. The combined multimodal imaging provided in the same experiment information on *in vivo* location (MRI) and viability (BLI) as well post-mortem cell fate (fluorescent label and histology) (Figure 4).

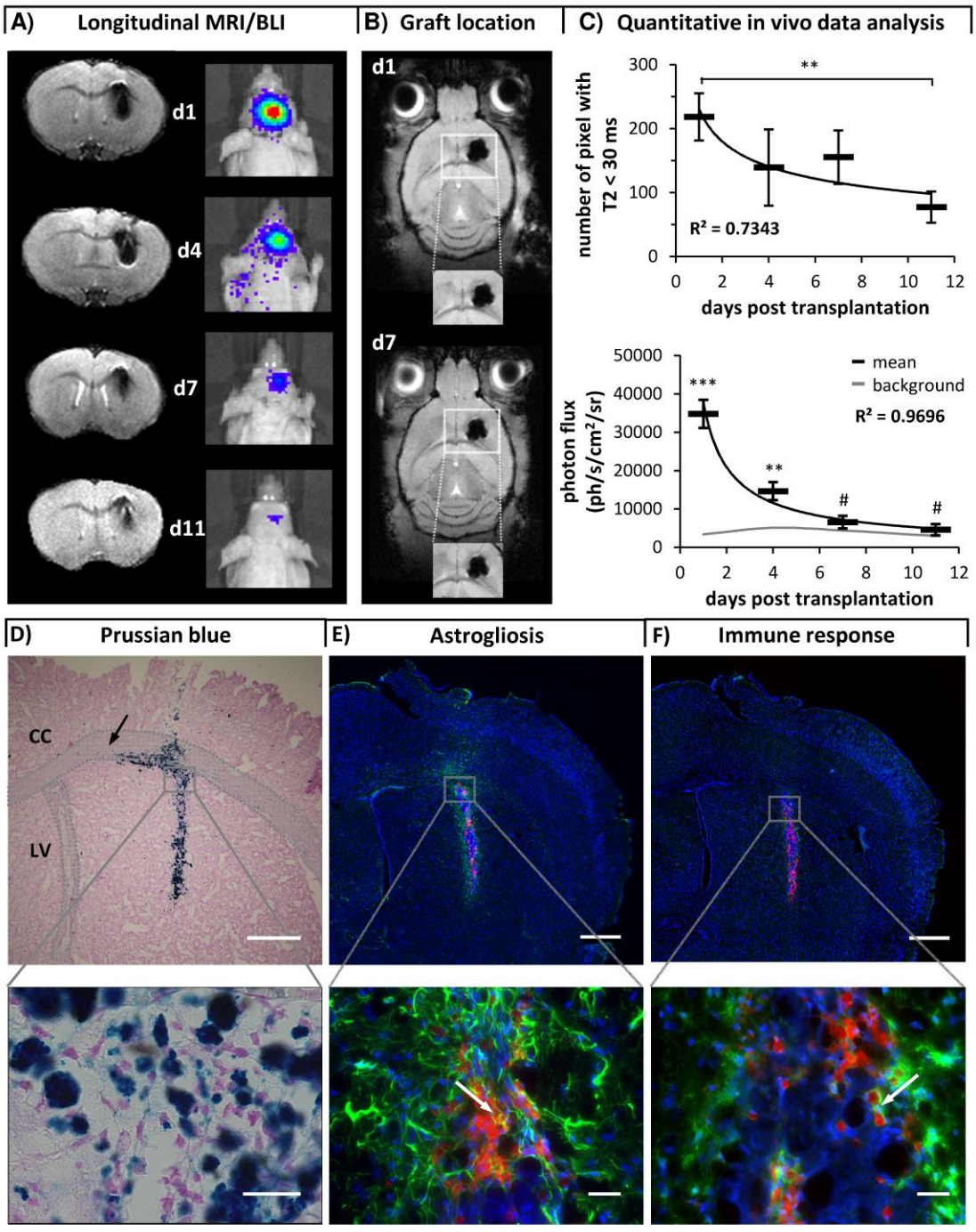


*Figure 4. Multimodal cell tracking of FTD-Vio594 labeled human neural stem cells in vivo and immuunohistochemical staining of the cell graft in host environment 11 days after transplantation.(A) Representative T2-weighted MRIs (coronal slices) and bioluminescence images (top view) acquired at 1, 4, 7 and 11 days post-transplantation of 150,000 human NSCs + FTD-Vio594 into the striatum. BLI data scaled with 1–10x10e4 ph /s /cm2/sr. (B) No MRI-detectable change of graft location or migration of cells as indicated by representative horizontal plane T2*-weighted MRIs from day 1 and 7. (C) Temporal profile of changes in number of hypointense pixels (T2 <30 ms) per hemisphere and photon flux from viable cells measured between day 1 and 14 upon transplantation. *p < 0.05; **p < 0.01; ***p < 0.001; #not significant. BLI: Bioluminescence imaging; CC: Corpus callosum; d: Day; FTD: FeraTrack Direct; LV: Lateral ventricle; NSC: Neural stem cell. From Aswendt et al (2015, their Figure 6), with permission.*

SPIOs have also been functionalized with antibodies for targeted labeling or cell sorting of neural stem cells (Peng et al., 2014), a procedure originally designed to target specific cell types with magnetic particle-conjugated antibodies (Miltenyi et al., 1990).

A challenge for MRI-based cell tracking is the unambiguous distinction of PP/SPP-labeled cells from small vessels due to the same negative contrast induced by both sources. Himmelreich and colleagues developed a method based on carbogen inhalation that allows a reliable discrimination of labelled stem cells from small vessels passing through the imaged brain tissue (Himmelreich et al., 2005). An additional complication can arise when activated microglia and macrophages engulf PP/SPP-labeled cells or released PP/SPPs and create signals unrelated to the originally labeled cells (Cupaioli et al., 2014). Another challenge is detection sensitivity. Recently, Zheng et al. used Magnetic Particle Imaging (MPI), which detects the intense magnetization of SPIOs directly rather than indirectly through local effects on surrounding water molecules, to track the fate of human NPCs injected into rat forebrain (Zheng et al., 2015). MPI provided higher sensitivity, but at 5-10x lower image resolution (1 mm with 7T/m magnetic gradient).

**Stroke**

Stroke remains a leading cause of death and disability worldwide. Although acute treatment has improved, no therapy exists to improve long-term recovery. As a result, many patients end up with lifelong disabilities. Stem cell injection has been shown to promote functional recovery in animal models through the induction of dendritic branching and synapse formation, enhanced neurogenesis and angiogenesis, and blood-brain barrier repair (Adamczak et al., 2017; Adamczak and Hoehn, 2015; Andres et al., 2011; Liu et al., 2008). The utility of MRI-based cell tracking in connection with stem cell therapy for stroke fulfills two purposes: 1) the stroke lesion can be visualized and assessed with clinically-relevant parameters of T1, T2, diffusion and perfusion, and 2) in the same imaging session, a high-resolution

T2/T2*-weighted sequence can be used to image PP/SPP-labelled cells (reviewed in Modo et al., 2005; Ramos-Cabrer and Hoehn, 2012).

**Parkinson's disease**

In contrast to stroke, which affects different neuronal cell types indiscriminately, in Parkinson's disease the primary damage is relatively selective, on a well-defined cell type. Cell therapy can therefore be targeted to replace nigrostriatal dopaminergic neurons, which has been shown to ameliorate motor symptoms such as rigidity, poverty of movement, tremor and postural instability (Lindvall and Kokaia, 2006). Several types of stem and progenitor cells have been proposed in this connection, and PP/SPP-labelling has been employed in some studies for *in vivo* tracking. Ramos-Gomez at al. tracked SPION-labelled immortalized human NSCs for up to 5 months after implantation into the affected sites of the rat brain. However, histological analyses showed that the PP/SPPs had accumulated in areas containing activated microglia, and co-localized with these, suggesting that either the implanted cells or PP/SPPs expelled from them had been internalized by host microglia (Ramos-Gómez et al. 2015).

Successful labeling with PP/SPPs has also been demonstrated for human fetal mesencephalic neural precursor cells (fmNPCs) and human NSCs overexpressing Bcl-XL (Boulland et al 2012) (Ramos-Gomez and Martinez-Serrano, 2016; Ramos-Gomez et al., 2015). However, the choice of PP/SPP type may be important, as effects of labeling on neuronal differentiation and function differ. Imam et al. (Imam et al., 2015) labeled a human neuroblastoma line with SPIONs (1 nm diameter) for 24 hours, and reported inhibition of cell-proliferation, significant reduction in the number of active mitochondria, and a dose-dependent increase in ROS. By contrast, labeling of fmNPCs with MPIOs led to no adverse effects on differentiation of the dopaminergic phenotype or on electrophysiological properties *in vitro* (Boulland et al 2012).

**Multiple Sclerosis**

Cell replacement therapy in multiple sclerosis (MS) aims to replenish lost myelin by replacing oligodendrocytes damaged by autoimmune reaction. The resultant symptoms vary depending on the location of the attack, and can include double vision, partial blindness, muscle weakness, loss of sensation, paresthesis or neuropathic pain, and tremor. Politi et al. labeled NPCs with 3 different commercially available SPIOs and injected the pre-labeled cells into the CNS of mice with experimental autoimmune encephalomyelitis (EAE), an animal model of MS (Politi et al., 2007). They verified by quantitative MRI and histology that the transplanted NPCs accumulated at inflammatory lesion sites and could be detected up to 20 days post-injection. Another imaging approach relevant to MS is based on the characteristic presence of phagocytic macrophages at MS lesion sites. Macrophages can therefore be labeled with PP/SPPs and injected intravenously, and subsequent MRI can be used to localize and define the extent of the inflammatory demyelination as well as dynamic changes resulting from immunosuppressive or other therapies (Muja and Bulte, 2009).

**Brain tumors**

Animal studies using PP/SPP-labeled glioblastoma cells have provided dynamic images of brain tumor progression and invasion. Similarly to the application of cell tracking in MS, the homing of transplanted stem cells to brain tumors has also been visualized by MRI-based stem cell tracking. Zhang et al. transplanted NPCs and mesenchymal stem cells (MSCs) pre-labeled with lipophilic dye-coated SPIOs into the cisterna magna of rats with a glioblastoma. They verified by histology the MRI detection of grafted cells that targeted and infiltrated the tumor (Zhang et al., 2004). More recent studies confirmed the high potential of MRI-based stem cell tracking for novel tumor therapies with different human MSC and NSC cell lines and contrast agents (Chaumeil et al., 2012; Thu et al., 2009). In a different approach, Elvira et al. labeled endogenous NSCs with targeted glyconanoparticles and followed their migration towards the site of a tumor in the mouse brain (Elvira et al., 2012). The water-soluble magnetic glyconanoparticles consisted of a 4nm magnetic core covered with a 1nm gold shell coated with carbohydrates and an amphiphilic linker

to an anti-Nilo2 antibody, which targets NPCs. PP/SPPs may be also introduced into the vicinity of a tumor for directed therapeutics – such as intratumoral thermotherapy, based on thermal activation of PP/SPPs with an alternating magnetic field, which heats up the particles causing cell death (Jordan et al., 2006).

**C. Clinical studies**

PP/SPP-labelled stem cells have been used in clinical studies investigating treatments for neurodegenerative diseases, stroke and ischemic damage, brain trauma and chronic spinal cord injury. Feridex-labeled autologous MSCs have been intravenously or intrathecally administrated to patients with MS and amyotrophic lateral sclerosis (ALS). Side effects and cell migration were followed for an extended time and the procedure was deemed both feasible and relatively safe, although there were acute immunomodulatory effects (Karussis et al. 2010). For stroke, more than 35 clinical trials are currently underway (George and Steinberg, 2015), with good indications of overall safety (12 months of follow-up) and recovery of motor function for a human stem cell line transplanted into chronic stroke patients (Steinberg et al., 2016). Janowski et al. report long-term clinical tracking of SPIO-labeled umbilical cord blood-derived stem cells after intracerebroventricular transplantation in a patient with global cerebral ischemia (Janowski et al., 2014). Labelled cells were still detectable after 4 months. Feridex-labeled autologous NSCs have been injected into the left temporal lobe of a patient with brain trauma, who was then imaged by MRI weekly for 10 weeks. The NSCs accumulated initially at the site of injection, and then over the course of 2-3 weeks migrated from there to periphery of the damaged brain tissue. Loss of signal after 7 weeks was attributed to dilution of PP/SPPs due to cell proliferation (Zhu et al. 2006). Autologous bone marrow-derived MSCs have been delivered intrathecally in patients with chronic spinal cord injury. Magnetic beads coated with monoclonal antibodies against the cell membrane antigen CD34 were used to label the cells prior to administration. The labelled cells migrated into the injured region of the spinal cord, but potential therapeutic effects were not assessed (Callera and de Melo 2007).

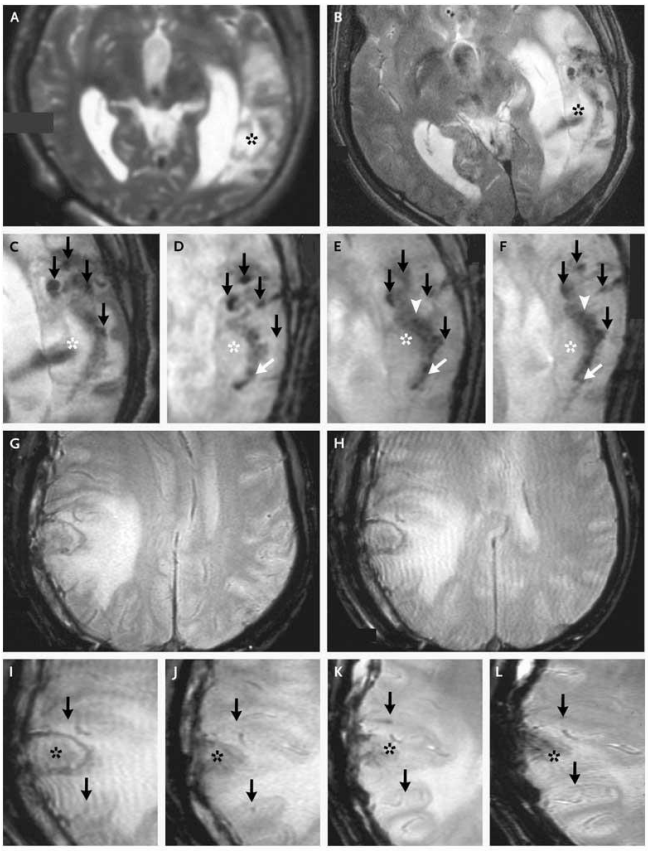


*Figure 5. MRI scans from the patient who received neural stem cells labeled with iron oxide nanoparticles (Panels A through F) and the patient who received unlabeled cells (Panels G through L). The scan obtained before the implantation of the labeled neural stem cells (Panel A) did not show a pronounced hypointense signal around the lesion (asterisk) in the left temporal lobe, whereas circular areas of hypointense signal were visible at the injection sites 1 day after implantation (Panel B). Magnified images are shown in Panels C through F. Four hypointense signals (black arrows) were observed at injection sites around the lesion on day 1 (Panel C), day 7 (Panel D), day 14 (Panel E), and day 21 (Panel F). On day 7 (Panel D), we observed dark signals (white arrow) posterior to the lesion, a finding that was consistent with the presence of the labeled cells. By day 14 (Panel E), the hypointense signals at the injection sites had faded, and another dark signal (white arrowhead) had appeared and spread along the border of the damaged brain tissue. By day 21 (Panel F), the dark signal had thickened and extended further along the lesion (white arrow). The scans in Panels G and H, from the patient who underwent implantation of unlabeled cells, were obtained on days 0 and 1, respectively, and the magnified views in Panels I, J, K, and L were obtained on days 1, 7, 14, and 21, respectively. A slightly hypointense signal is present around the injection sites in Panels I, J, K, and L. In these panels, the black arrows indicate the hypointense signal, and the asterisks indicate the lesion. From Zhu J et al. (2006, their Figure 2), with permission*.

## VI. Summary

The advent of cell-based therapies and rapid advances in stem cell technology highlight the need to develop robust, reliable and clinically viable methods for

tracking the fate of stem cells, progenitor cells and other cell types within the human body and in preclinical animal models. Although fluorescence- and luminescence-based tracking can be used at cellular resolution in small animals, depth constraints render them practically useless in large animals and humans. Achieving similar spatial resolution at depth can really only be obtained at present with magnetic resonance imaging. For this reason, developing cellular labeling approaches with paramagnetic/superparamagnetic particles has become an important area of research aimed at providing valid cell tracking in patients.

A wide variety of PP/SPPs have been and are being developed that are beginning to meet this aim in the context of cardiological and neurological disease. Key issues include the reliability with which different types of cells can be labeled with PP/SPPs, the effects of this labeling on cell health and function, strategies for implantation in the heart and brain, potential long term effects *in vivo* and the extent to which PP/SPP-labeling can be made suitably transient, and the problems associated with unintended loss of PP/SPPs from labeled cells and scavenging by peregrinating macrophages and microglia. Numerous studies indicate that many existing PP/SPPs can be utilized without seriously compromising cardiac or neural cell function, although the potential for adverse effects of excess iron must be weighed carefully. PP/SPPs, through diverse schemes of functionalization, also provide many opportunities for combining MRI visualization with molecular manipulation of the labeled cells.

As the development of PP/SPPs and their *in vivo* imaging advances, and assuming remaining issues can be resolved, we expect that their clinical use in cardiological and neurological disease will become a reality. Non-invasive imaging of PP/SPP-labeled cells will then become an important tool in assessing and controlling cell implantation therapies.

**Acknowledgements**

JCG and JLB are supported by the Norwegian Research Council (grants 230000, 189374, 229654) and the Southeastern Norway Health Authority (grants 2011035, 2015045, 2015102, 2014119). MP and JL are supported by ARRS grants J7-7424, Z4-8229 and P1-0055. DM is supported by the Croatian Science Foundation (IP-2016-06-9451) and co-financed by the European Union through the European Regional Development Fund, Operational Programme Competitiveness and Cohesion, grant agreement No. KK.01.1.1.01.0007, CoRE – Neuro.

**References**

Aboody KS, Brown A, Rainov NG, et al (2000) Neural stem cells display extensive tropism for pathology in adult brain: evidence from intracranial gliomas. Proc Natl Acad Sci U S A 97:12846–12851. doi: 10.1073/pnas.97.23.12846

Adamczak J, Aswendt M, Kreutzer C, Rotheneichner P, Riou A, Selt M, et al. Neurogenesis upregulation on the healthy hemisphere after stroke enhances compensation for age-dependent decrease of basal neurogenesis. Neurobiol Dis. 2017;99:47-57. Epub 2016/12/23. doi: 10.1016/j.nbd.2016.12.015. PubMed PMID: 28007584

Adamczak J, Hoehn M. Poststroke angiogenesis, con: dark side of angiogenesis. Stroke. 2015;46(5):e103-4. Epub 2015/03/31. doi: 10.1161/STROKEAHA.114.007642. PubMed PMID: 25813195.

Adams CF, Rai A, Sneddon G, et al (2015) Increasing magnetite contents of polymeric magnetic particles dramatically improves labeling of neural stem cell transplant populations. Nanomedicine Nanotechnol Biol Med 11:19–29. doi: 10.1016/j.nano.2014.07.001

Afridi MJ, Ross A, Liu X, Bennewitz MF, Shuboni DD, Shapiro EM. Intelligent and automatic in vivo detection and quantification of transplanted cells in MRI. Magn Reson Med. 2017 Nov;78(5):1991-2002. doi: 10.1002/mrm.26571.

Aguirre P, Natalia P. Mena, Carlos M. Carrasco, Yorka Muñoz, Patricio Pérez-Henríquez, Rodrigo A. Morales, Bruce K. Cassels, Carolina Méndez-Gálvez, Olimpo García-Beltrán, Christian González-Billault, Marco T. Núñez. Iron Chelators and Antioxidants Regenerate Neuritic Tree and Nigrostriatal Fibers of MPP/SPP+/MPTP-Lesioned Dopaminergic Neurons
PLoS One. 2015; 10(12): e0144848. Published online 2015 Dec 14. doi: 10.1371/journal.pone.0144848

Ahrens ET, Feili-Hariri M, Xu H, Genove G, Morel A. Receptor mediated endocytosis of iron-oxide particles provides efficient labeling of dendritic cells for in vivo MR imaging. Magn Reson Med 2003;49:1006–1013.

Akinc and Battaglia 2013
https://cshperspectives.cshlp.org/content/5/11/a016980.full

Alam SR, Stirrat C, Spath N, Zamvar V, Pessotto R, Dweck MR, Moore C, Semple S, El-Medany A, Manoharan D, Mills NL, Shah A, Mirsadraee S, Newby DE, Henriksen PA. Myocardial inflammation, injury and infarction during on-pump coronary artery bypass graft surgery. J Cardiothorac Surg. 2017 Dec 16;12(1):115

Albers, J., Pacilé, S., Markus, M., Wiart, M., Vande Velde, G., Tromba, G., Dullin, C., 2018. X-ray-based 3D virtual histology - adding the next dimension to histological analsysis. Molecular Imaging and Biology.

Ali LMA, Piñol R, Villa-Bellosta R, et al (2015) Cell compatibility of a maghemite/polymer biomedical nanoplatform. Toxicol Vitro Int J Publ Assoc BIBRA 29:962–975. doi: 10.1016/j.tiv.2015.04.003

Amado LC, Saliaris AP, Schuleri KH, et al (2005) Cardiac repair with intramyocardial injection of allogeneic mesenchymal stem cells after myocardial infarction. Proc Natl Acad Sci U S A 102:11474–11479. doi: 10.1073/pnas.0504388102

Amsalem Y, Mardor Y, Feinberg MS, et al (2007) Iron-oxide labeling and outcome of transplanted mesenchymal stem cells in the infarcted myocardium. Circulation 116:I38-45. doi: 10.1161/CIRCULATIONAHA.106.680231

Amstad E, Zurcher S, Mashaghi A, Wong JY, Textor M, Reimhult E. (2009) Surface functionalization of single superparamagnetic iron oxide nanoparticles for targeted magnetic resonance imaging. Small. 2009 Jun;5(11):1334-42. doi: 10.1002/smll.200801328.

Andersen AJ, Windschiegl B, Ilbasmis-Tamer S, et al (2013) Complement activation by PEG-functionalized multi-walled carbon nanotubes is independent of PEG molecular mass and surface density. Nanomedicine Nanotechnol Biol Med 9:469–473. doi: 10.1016/j.nano.2013.01.011

Andjus PR, Bataveljić D, Vanhoutte G, Mitrecic D, Pizzolante F, Djogo N, Nicaise C, Gankam Kengne F, Gangitano C, Michetti F, van der Linden A, Pochet R, Bacić G. In vivo morphological changes in animal models of amyotrophic lateral sclerosis and Alzheimer's-like disease: MRI approach. Anat Rec (Hoboken). 2009;292(12):1882-92. doi: 10.1002/ar.20995. PubMed PMID: 19943341.

Andres RH, Horie N, Slikker W, Keren-Gill H, Zhan K, Sun G, et al. Human neural stem cells enhance structural plasticity and axonal transport in the ischaemic brain. Brain. 2011;134(Pt 6):1777-89. Epub 2011/05/28. doi: 10.1093/brain/awr094. PubMed PMID: 21616972; PubMed Central PMCID: PMCPMC3102243.

Arai T, Kofidis T, Bulte JWM, et al (2006) Dual in vivo magnetic resonance evaluation of magnetically labeled mouse embryonic stem cells and cardiac function at 1.5 t. Magn Reson Med 55:203–209. doi: 10.1002/mrm.20702

Arbab AS, Bashaw LA, Miller BR, et al (2003a) Characterization of biophysical and metabolic properties of cells labeled with superparamagnetic iron oxide nanoparticles and transfection agent for cellular MR imaging. Radiology 229:838–846. doi: 10.1148/radiol.2293021215

Arbab AS, Bashaw LA, Miller BR, et al (2003b) Intracytoplasmic tagging of cells with ferumoxides and transfection agent for cellular magnetic resonance imaging after cell transplantation: methods and techniques. Transplantation 76:1123–1130. doi: 10.1097/01.TP.0000089237.39220.83

Arbab AS, Wilson LB, Ashari P, et al (2005a) A model of lysosomal metabolism of dextran coated superparamagnetic iron oxide (SPIO) nanoparticles: implications for cellular magnetic resonance imaging. NMR Biomed 18:383–389. doi: 10.1002/nbm.970

Arbab AS, Yocum GT, Kalish H, et al (2004) Efficient magnetic cell labeling with protamine sulfate complexed to ferumoxides for cellular MRI. Blood 104:1217–1223. doi: 10.1182/blood-2004-02-0655

Arbab AS, Yocum GT, Rad AM, et al (2005b) Labeling of cells with ferumoxides-protamine sulfate complexes does not inhibit function or differentiation capacity of hematopoietic or mesenchymal stem cells. NMR Biomed 18:553–559. doi: 10.1002/nbm.991

Aswendt M, Henn N, Michalk S, Schneider G, Steiner MS, Bissa U, et al. Novel bimodal iron oxide particles for efficient tracking of human neural stem cells in vivo. Nanomedicine (Lond). 2015;10(16):2499-512. Epub 2015/08/22. doi: 10.2217/NNM.15.94. PubMed PMID: 26296195.

Au K-W, Liao S-Y, Lee Y-K, et al (2009) Effects of iron oxide nanoparticles on cardiac differentiation of embryonic stem cells. Biochem Biophys Res Commun 379:898–903. doi: 10.1016/j.bbrc.2008.12.160

Ayala V, Herrera AP, Latorre-Esteves M, et al (2013) Effect of surface charge on the colloidal stability and in vitro uptake of carboxymethyl dextran-coated iron oxide nanoparticles. J Nanoparticle Res 15:1874. doi: 10.1007/s11051-013-1874-0

Ayton S, Lei P (2014) Nigral iron elevation is an invariable feature of Parkinson's disease and is a sufficient cause of neurodegeneration. BioMed Res Int 2014:581256. doi: 10.1155/2014/581256

Bajetto A, Barbieri F, Dorcaratto A, et al (2006) Expression of CXC chemokine receptors 1-5 and their ligands in human glioma tissues: role of CXCR4 and SDF1 in glioma cell proliferation and migration. Neurochem Int 49:423–432. doi: 10.1016/j.neuint.2006.03.003

Banda NK, Mehta G, Chao Y, et al (2014) Mechanisms of complement activation by dextran-coated superparamagnetic iron oxide (SPIO) nanoworms in mouse versus human serum. Part Fibre Toxicol 11:64. doi: 10.1186/s12989-014-0064-2

Bareford LM, Swaan PW (2007) Endocytic mechanisms for targeted drug delivery. Adv Drug Deliv Rev 59:748–758. doi: 10.1016/j.addr.2007.06.008

Barrow M, Taylor A, Murray P, et al (2015) Design considerations for the synthesis of polymer coated iron oxide nanoparticles for stem cell labelling and tracking using MRI. Chem Soc Rev 44:6733–6748. doi: 10.1039/c5cs00331h

Bataveljić D, Djogo N, Zupunski L, Bajić A, Nicaise C, Pochet R, Bacić G, Andjus PR. Live monitoring of brain damage in the rat model of amyotrophic lateral sclerosis. Gen Physiol Biophys. 2009;28 Spec No:212-8. PubMed PMID:19893103.

Bengel FM. Issue "noninvasive molecular imaging and theranostic probes": New concepts in myocardial imaging. Methods. 2017 Nov 1;130:72-78

Ben-Hur T, van Heeswijk RB, Einstein O, et al (2007) Serial in vivo MR tracking of magnetically labeled neural spheres transplanted in chronic EAE mice. Magn Reson Med 57:164–171. doi: 10.1002/mrm.21116

Berman SC, Galpoththawela C, Gilad AA, Bulte JW, Walczak P. Long-term MR cell tracking of neural stem cells grafted in immunocompetent versus immunodeficient mice reveals distinct differences in contrast between live and dead cells. Magn Reson Med. 2011;65(2):564-74. Epub 2010/10/12. doi: 10.1002/mrm.22613. PubMed PMID: 20928883; PubMed Central PMCID: PMCPMC3031985.

Bobo D, Robinson KJ, Islam J, et al (2016) Nanoparticle-Based Medicines: A Review of FDA-Approved Materials and Clinical Trials to Date. Pharm Res 33:2373–2387. doi: 10.1007/s11095-016-1958-5

Boulland JL, Leung DS, Thuen M, Vik-Mo E, Joel M, Perreault MC, Langmoen IA, Haraldseth O, Glover JC. Evaluation of intracellular labeling with micron-sized particles of iron oxide (MPIOs) as a general tool for in vitro and in vivo tracking of human stem and progenitor cells. Cell Transplant. 2012;21(8):1743-59. doi: 10.3727/096368911X627598.

Bregar VB, Lojk J, Šuštar V, et al (2013) Visualization of internalization of functionalized cobalt ferrite nanoparticles and their intracellular fate. Int J Nanomedicine 8:919–931. doi: 10.2147/IJN.S38749

Bulte JW, Vymazal J, Brooks RA, et al (1993) Frequency dependence of MR relaxation times. II. Iron oxides. J Magn Reson Imaging JMRI 3:641–648

Bulte JW, Zhang S, van Gelderen P, Herynek V, Jordan EK, Duncan ID, Frank JA. Neurotransplantation of magnetically labeled oligodendrocyte progenitors: magnetic resonance tracking of cell migration and myelination. Proc Natl Acad Sci USA 1999;96:15256–15261.

Bulte JW, Douglas T, Witwer B, et al (2001) Magnetodendrimers allow endosomal magnetic labeling and in vivo tracking of stem cells. Nat Biotechnol 19:1141–1147. doi: 10.1038/nbt1201-1141

Bulte JWM, Kraitchman DL, Mackay AM, Pittenger MF (2004) Chondrogenic differentiation of mesenchymal stem cells is inhibited after magnetic labeling with ferumoxides. Blood 104:3410–3412; author reply 3412-3413. doi: 10.1182/blood-2004-06-2117

Busquets MA, Alba Espargaró, Raimon Sabaté, Joan Estelrich. Magnetic Nanoparticles Cross the Blood-Brain Barrier: When Physics Rises to a Challenge Nanomaterials (Basel) 2015 Dec; 5(4): 2231–2248. Published online 2015 Dec 11. doi: 10.3390/nano5042231. PMCID: PMC5304810

Callera F, de Melo CMTP (2007) Magnetic resonance tracking of magnetically labeled autologous bone marrow CD34+ cells transplanted into the spinal cord via lumbar puncture technique in patients with chronic spinal cord injury: CD34+ cells' migration into the injured site. Stem Cells Dev 16:461–466. doi: 10.1089/scd.2007.0083

Cengelli F, Maysinger D, Tschudi-Monnet F, Montet X, Corot C, Petri-Fink A, Hofmann H, Juillerat-Jeanneret L. Interaction of functionalized superparamagnetic iron oxide nanoparticles with brain structures. J Pharmacol Exp Ther. 2006 Jul; 318(1):108-16.

Cengelli F, Voinesco F, Juillerat-Jeanneret L (2010) Interaction of cationic ultrasmall superparamagnetic iron oxide nanoparticles with human melanoma cells. Nanomed 5:1075–1087. doi: 10.2217/nnm.10.79

Chang J, Jallouli Y, Kroubi M, et al (2009) Characterization of endocytosis of transferrin-coated PLGA nanoparticles by the blood–brain barrier. Int J Pharm 379:285–292. doi: 10.1016/j.ijpharm.2009.04.035

Chanmee T, Ontong P, Konno K, Itano N (2014) Tumor-Associated Macrophages as Major Players in the Tumor Microenvironment
Cancers (Basel). 2014 Sep; 6(3): 1670–1690.
Published online 2014 Aug 13. doi: 10.3390/cancers6031670

Chaumeil MM, Gini B, Yang H, Iwanami A, Sukumar S, Ozawa T, et al. Longitudinal evaluation of MPIO-labeled stem cell biodistribution in glioblastoma using high resolution and contrast-enhanced MR imaging at 14.1 tesla. Neuro Oncol. 2012;14(8):1050-61. Epub 2012/06/07. doi: 10.1093/neuonc/nos126.

Chen C, Vat V, Termglinchan IK. Concise Review: Mending a Broken Heart: The Evolution of Biological Therapeutics. STEM CELLS 2017;35:1131–1140).

Chen F, Wang G, Griffin JI, et al (2016) Complement proteins bind to nanoparticle protein corona and undergo dynamic exchange in vivo. Nat Nanotechnol advance online publication: doi: 10.1038/nnano.2016.269

Chen J, Yang J, Liu R, Qiao C, Lu Z, Shi Y, Fan Z, Zhang Z, Zhang X(1). Dual-targeting Theranostic System with Mimicking Apoptosis to Promote Myocardial Infarction Repair via Modulation of Macrophages.Theranostics. 2017 Sep 26;7(17):4149-4167

Chen Y-C, Hsiao J-K, Liu H-M, et al (2010) The inhibitory effect of superparamagnetic iron oxide nanoparticle (Ferucarbotran) on osteogenic differentiation and its signaling mechanism in human mesenchymal stem cells. Toxicol Appl Pharmacol 245:272–279. doi: 10.1016/j.taap.2010.03.011

Cianciaruso C, Pagani A, Martelli C, Bacigaluppi M, Squadrito ML, Lo Dico A, et al. Cellular magnetic resonance with iron oxide nanoparticles: long-term persistence of SPIO signal in the CNS after transplanted cell death. Nanomedicine (Lond). 2014;9(10):1457-74. Epub 2014/05/16. doi: 10.2217/nnm.14.84.

Cohen ME, Muja N, Fainstein N, et al (2010) Conserved fate and function of ferumoxides-labeled neural precursor cells in vitro and in vivo. J Neurosci Res 88:936–944. doi: 10.1002/jnr.22277

Contag, C. H.; Bachmann, M. H. Advances in in vivo bioluminescence imaging of gene expression. Annu. Rev. Biomed. Eng. 4:235–260; 2002.

Crabbe A, Vandeputte C, Dresselaers T, Sacido AA, Verdugo JM, Eyckmans J, et al. Effects of MRI contrast agents on the stem cell phenotype. Cell Transplant. 2010;19(8):919-36. Epub 2010/03/31. doi: 10.3727/096368910X494623.

Cromer Berman SM, Walczak P, Bulte JWM (2011) Tracking stem cells using magnetic nanoparticles. Wiley Interdiscip Rev Nanomed Nanobiotechnol 3:343–355. doi: 10.1002/wnan.140

Cromer Berman SM, Kshitiz, Wang CJ, Orukari I, Levchenko A, Bulte JW, et al. Cell motility of neural stem cells is reduced after SPIO-labeling, which is mitigated after exocytosis. Magn Reson Med. 2013;69(1):255-62. Epub 2012/03/01. doi: 10.1002/mrm.24216.

Cupaioli FA, Zucca FA, Boraschi D, Zecca L. Engineered nanoparticles. How brain friendly is this new guest? Prog Neurobiol. 2014;119-120:20-38. Epub 2014/05/14. doi: 10.1016/j.pneurobio.2014.05.002.

de Kemp, R. A.; Epstein, F. H.; Catana, C.; Tsui, B. M. W.; Ritman, E. L. Small-animal molecular imaging methods. J. Nucl. Med. 51(suppl 5):18S–32S; 2010.

De Palma R, Trekker J, Peeters S, Van Bael MJ, Bonroy K, Wirix-Speetjens R, Reekmans G, Laureyn W, Borghs G, Maes G (2007) Surface modification of gamma-Fe2O3@SiO2 magnetic nanoparticles for the controlled interaction with biomolecules. J Nanosci Nanotechnol. 2007 Dec;7(12):4626-41.

Deng, Z.J. Nanoparticle-induced unfolding of fibrinogen promotes Mac-1 receptor activation and inflammation. *Nat. Nanotechnol.* **6**, 39–44 (2011)

Desestret V, Brisset J-C, Moucharrafie S, et al (2009) Early-stage investigations of ultrasmall superparamagnetic iron oxide-induced signal change after permanent middle cerebral artery occlusion in mice. Stroke 40:1834–1841. doi: 10.1161/STROKEAHA.108.531269

Detante O, Valable S, de Fraipont F, et al (2012) Magnetic resonance imaging and fluorescence labeling of clinical-grade mesenchymal stem cells without impacting

their phenotype: study in a rat model of stroke. Stem Cells Transl Med 1:333–341. doi: 10.5966/sctm.2011-0043

Diana V, Bossolasco P, Moscatelli D, et al (2013) Dose Dependent Side Effect of Superparamagnetic Iron Oxide Nanoparticle Labeling on Cell Motility in Two Fetal Stem Cell Populations. PLoS ONE 8:. doi: 10.1371/journal.pone.0078435

Dib N, Menasche P, Bartunek JJ, Zeiher AM, Terzic A, Chronos NA, Henry TD, Peters NS, Fernández-Avilés F, Yacoub M, Sanborn TA, Demaria A, Schatz RA, Taylor DA, Fuchs S, Itescu S, Miller LW, Dinsmore JH, Dangas GD, Popma JJ, Hall JL, Holmes DR Jr; International Society for Cardiovascular Translational Research. Recommendations for successful training on methods of delivery of biologics for cardiac regeneration: a report of the International Society for Cardiovascular Translational Research. JACC Cardiovasc Interv. 2010 Mar;3(3):265-75

Doherty GJ, McMahon HT (2009) Mechanisms of endocytosis. Annu Rev Biochem 78:857–902. doi: 10.1146/annurev.biochem.78.081307.110540

Dringen R, Bishop GM, Koeppe M, et al (2007) The pivotal role of astrocytes in the metabolism of iron in the brain. Neurochem Res 32:1884–1890. doi: 10.1007/s11064-007-9375-0

Dousset V, Brochet B, Deloire MS, Lagoarde L, Barroso B, Caille JM, Petry KG. MR imaging of relapsing multiple sclerosis patients using ultra-small-particle iron oxide and compared with gadolinium. AJNR Am J Neuroradiol. 2006; 27(5):1000-5.

Elvira G, Garcia I, Benito M, Gallo J, Desco M, Penades S, et al. Live imaging of mouse endogenous neural progenitors migrating in response to an induced tumor. PLoS One. 2012;7(9):e44466. Epub 2012/09/08. doi: 10.1371/journal.pone.0044466. Eschenhagen T., et al Cardiomyocyte Regeneration: A Consensus Statement. Circulation. 2017;136:680-686; Menasché P. Cardiac cell therapy: lessons from clinical trials. J Mol Cell Cardiol 50: 258–265, 2011)

Florian A, Ludwig A, Rösch S, Yildiz H, Klumpp S, Sechtem U, Yilmaz A. Positive effect of intravenous iron-oxide administration on left ventricular remodelling in patients with acute ST-elevation myocardial infarction – a cardiovascular magnetic resonance (CMR) study. Int J Cardiol. 2014 May 1;173(2):184-9

Fadeel B, Fornara A, Toprak MS, Bhattacharya K (2015) Keeping it real: The importance of material characterization in nanotoxicology. Biochem Biophys Res Commun 468:498–503. doi: 10.1016/j.bbrc.2015.06.178

Farini A, Villa C, Manescu A, Fiori F, Giuliani A, Razini P, Sitzia C, Del Fraro G, Belicchi M, Meregalli M, Rustichelli F, Torrente Y. Novel insight into stem cell trafficking in dystrophic muscle, Int J Nanomed 2012; 7: 3059–3067.

Focke A, Schwarz S, Foerschler A, et al (2008) Labeling of human neural precursor cells using ferromagnetic nanoparticles. Magn Reson Med 60:1321–1328. doi: 10.1002/mrm.21745

Frangioni JV and Hajjar RJ. In Vivo Tracking of Stem Cells for Clinical Trials in Cardiovascular Disease. Circulation 2004;110;3378-3383

Frank JA, Miller BR, Arbab AS, et al (2003) Clinically applicable labeling of mammalian and stem cells by combining superparamagnetic iron oxides and transfection agents. Radiology 228:480–487. doi: 10.1148/radiol.2281020638

Frank JA, Kalish H, Jordan EK, Anderson SA, Pawelczyk E, Arbab AS. Color transformation and fluorescence of Prussian blue-positive cells: implications for histologic verification of cells labeled with superparamagnetic iron oxide nanoparticles. Mol Imaging. 2007;6(3):212-8. Epub 2007/05/30.

Freeman SA, Grinstein S (2014) Phagocytosis: receptors, signal integration, and the cytoskeleton. Immunol Rev 262:193–215. doi: 10.1111/imr.12212

Fu Y., Kraitchman D.L. Stem cell labeling for noninvasive delivery and tracking in cardiovascular regenerative therapy. Expert Rev Cardiovasc Ther, 8 (8) (2010), 1149-1160

Fujiwara N, Kobayashi K. Macrophages in inflammation. Curr Drug Targets Inflamm Allergy. 2005 Jun;4(3):281-6.

Gallo J, Long NJ, Aboagye EO (2013) Magnetic nanoparticles as contrast agents in the diagnosis and treatment of cancer. Chem Soc Rev 42:7816. doi: 10.1039/c3cs60149h

Garot J, Unterseeh T, Teiger E, et al (2003) Magnetic resonance imaging of targeted catheter-based implantation of myogenic precursor cells into infarcted left ventricular myocardium. J Am Coll Cardiol 41:1841–1846.

Geppert M, Hohnholt MC, Nürnberger S, Dringen R (2012) Ferritin up-regulation and transient ROS production in cultured brain astrocytes after loading with iron oxide nanoparticles. Acta Biomater 8:3832–3839. doi: 10.1016/j.actbio.2012.06.029

Geppert M, Hohnholt MC, Thiel K, et al (2011) Uptake of dimercaptosuccinate-coated magnetic iron oxide nanoparticles by cultured brain astrocytes. Nanotechnology 22:145101. doi: 10.1088/0957-4484/22/14/145101

George PM, Steinberg GK. Novel Stroke Therapeutics: Unraveling Stroke Pathophysiology and Its Impact on Clinical Treatments. Neuron. 2015;87(2):297-309. Epub 2015/07/17. doi: 10.1016/j.neuron.2015.05.041.

Gerber TC et al. Ionizing Radiation in Cardiac Imaging. A Science Advisory From the American Heart Association Committee on Cardiac Imaging of the Council on Clinical Cardiology and Committee on Cardiovascular Imaging and Intervention of the

Council of Cardiovascular Radiology and Intervention DOI:10.1161/CIRCULATION AHA.108.191650 february 2009

Glover, J. C. (1995) Retrograde and anterograde axonal tracing with fluorescent dextrans in the embryonic nervous system. Neuroscience Protocols 30:1-13.

Glover JC (2014) Conjugated dextran amines as intracellular tracers for visualizing and manipulating neurons. In: Dextran: Chemical Structure, Applications and Potential Side Effects. Recent Trends in Biotechnology.
Ed: Garrett P. Figgs. Nova Publishers, Hauppauge, NY. pp. 157-174. ISBN: 978-1-62948-960-5.

Giuliani A, Frati C, Rossini A, Komlev VS, Lagrasta C, Savi M, Cavalli S, Gaetano C, Quaini F, Manescu A, Rustichelli F. High-resolution X-ray microtomography for three-dimensional imaging of cardiac progenitor cell homing in infarcted rat hearts. J Tissue Eng Regen Med. 2011 Feb 24.

Goodfellow F, Simchick GA, Mortensen LJ, et al (2016) Tracking and Quantification of Magnetically Labeled Stem Cells using Magnetic Resonance Imaging. Adv Funct Mater 26:3899–3915. doi: 10.1002/adfm.201504444

Grealish S, Diguet E, Kirkeby A, Mattsson B, Heuer A, Bramoulle Y, et al. Human ESC-derived dopamine neurons show similar preclinical efficacy and potency to fetal neurons when grafted in a rat model of Parkinson's disease. Cell Stem Cell. 2014;15(5):653-65. Epub 2014/12/18. doi: 10.1016/j.stem.2014.09.017.

Guo Y, Chen W, Wang W, Shen J, Guo R, Gong F, Lin S, Cheng D, Chen G, Shuai X. Simultaneous diagnosis and gene therapy of immuno-rejection in rat allogeneic heart transplantation model using a T-cell-targeted theranostic nanosystem. ACS Nano. 2012 Dec 21;6(12):10646-57

Gupta AK, Gupta M (2005) Synthesis and surface engineering of iron oxide nanoparticles for biomedical applications. Biomaterials 26:3995–4021. doi: 10.1016/j.biomaterials.2004.10.012

Gutiérrez L, Romero S, da Silva GB, et al (2015) Degradation of magnetic nanoparticles mimicking lysosomal conditions followed by AC susceptibility. Biomed Tech (Berl) 60:417–425. doi: 10.1515/bmt-2015-0043

Guzman R, Uchida N, Bliss TM, et al (2007) Long-term monitoring of transplanted human neural stem cells in developmental and pathological contexts with MRI. Proc Natl Acad Sci U S A 104:10211–10216. doi: 10.1073/pnas.0608519104

Gyöngyösi M, Haller PM, Blake DJ, Martin Rendon E. Meta-Analysis of Cell Therapy Studies in Heart Failure and Acute Myocardial Infarction. Circ Res. 2018 Jul 6;123(2):301-308)

Hainfeld, J., Slatkin, D., Focella, T., Smilowitz, H., 2006. Gold nanoparticles: a new x-ray contrast agent. British Journal of Radiology 79, 248-253.

Hawrylak N, Ghosh P, Broadus J, Schlueter C, Greenough WT, Lauterbur PC. Nuclear magnetic resonance (NMR) imaging of iron oxide-labeled neural transplants. Exp Neurol. 1993;121(2):181-92. PubMed PMID: 8339769.

Helmchen, F.; Denk, W. Deep tissue two-photon micros- copy. Nat. Methods 2(12):932–940; 2005.

Hentze MW, Muckenthaler MU, Andrews NC (2004) Balancing Acts: Molecular Control of Mammalian Iron Metabolism. Cell 117:285–297. doi: 10.1016/S0092-8674(04)00343-5

Heyn, C.; Ronald, J. A.; Ramadan, S. S.; Snir, J. A.; Barry, A. M.; MacKenzie, L. T.; Mikulis, D. J.; Palmieri, D.; Bronder, J. L.; Steeg, P. S.; Yoneda, T.; MacDonald, I. C.; Chambers, A. F.; Rutt, B. K.; Foster, P. J. In vivo MRI of cancer cell fate at the single-cell level in a mouse model of breast cancer metastasis to the brain. Magn. Reson. Med. 56(5):1001–1010; 2006.

Higashi Y, Kimura M, Hara K, et al. Autologous bone marrow mononuclear cell implantation improves endothelium- dependent vasodilation in patients with limb ischemia. Circulation 2004;109:1215–1218.

Hill JM, Dick AJ, Raman VK, et al (2003) Serial cardiac magnetic resonance imaging of injected mesenchymal stem cells. Circulation 108:1009–1014. doi: 10.1161/01.CIR.0000084537.66419.7A

Himes N, Min J-Y, Lee R, et al (2004) In vivo MRI of embryonic stem cells in a mouse model of myocardial infarction. Magn Reson Med 52:1214–1219. doi: 10.1002/mrm.20220

Himmelreich U, WEber R, Ramos-Cabrer P, Wegener S, Kandal K, Shapiro EM, et al. Improved stem cell MR detectability in animal models by modification of the inhalation gas. Molecular Imaging. 2005;4:104-9.

Hoehn M, Küstermann E, Blunk J, et al (2002) Monitoring of implanted stem cell migration in vivo: a highly resolved in vivo magnetic resonance imaging investigation of experimental stroke in rat. Proc Natl Acad Sci U S A 99:16267–16272. doi: 10.1073/pnas.242435499. PubMed PMID: 12444255; PubMed Central PMCID: PMCPMC138600

Hohnholt MC, Dringen R (2011) Iron-dependent formation of reactive oxygen species and glutathione depletion after accumulation of magnetic iron oxide nanoparticles by oligodendroglial cells. J Nanoparticle Res 13:6761–6774. doi: 10.1007/s11051-011-0585-7

Hohnholt MC, Dringen R (2013) Uptake and metabolism of iron and iron oxide nanoparticles in brain astrocytes. Biochem Soc Trans 41:1588–1592. doi: 10.1042/BST20130114

Hsiao J-K, Chu H-H, Wang Y-H, et al (2008) Macrophage physiological function after superparamagnetic iron oxide labeling. NMR Biomed 21:820–829. doi: 10.1002/nbm.1260

Huang D, Zhou H, Gao J (2015) Nanoparticles modulate autophagic effect in a dispersity-dependent manner. Sci Rep 5:14361. doi: 10.1038/srep14361

Huang PP, Li SZ, Han MZ, et al. Autologous transplantation of peripheral blood stem cells as an effective therapeutic approach for severe arteriosclerosis obliterans of lower extremities. Thromb Haemost 2004;91:606–609

Imam SZ, Lantz-McPeak SM, Cuevas E, et al (2015) Iron Oxide Nanoparticles Induce Dopaminergic Damage: In vitro Pathways and In Vivo Imaging Reveals Mechanism of Neuronal Damage. Mol Neurobiol 52:913–926. doi: 10.1007/s12035-015-9259-2. PubMed PMID: 26099304.

Iversen T-G, Skotland T, Sandvig K (2011) Endocytosis and intracellular transport of nanoparticles: Present knowledge and need for future studies. NanoToday 6:176-185. doi.org/10.1016/j.nantod.2011.02.003

Jacobs, R. E.; Cherry, S. R. Complementary emerging techniques: High-resolution PET and MRI. Curr. Opin. Neurobiol. 11(5):621–629; 2001.

Janowski M, Walczak P, Kropiwnicki T, Jurkiewicz E, Domanska-Janik K, Bulte JW, et al. Long-term MRI cell tracking after intraventricular delivery in a patient with global cerebral ischemia and prospects for magnetic navigation of stem cells within the CSF. PLoS One. 2014;9(2):e97631. Epub 2014/06/12. doi: 10.1371/journal.pone.0097631.

Jendelová P, Herynek V, DeCroos J, et al (2003) Imaging the fate of implanted bone marrow stromal cells labeled with superparamagnetic nanoparticles. Magn Reson Med 50:767–776. doi: 10.1002/mrm.10585

Jin R, Lin B, Li D, Ai H (2014) Superparamagnetic iron oxide nanoparticles for MR imaging and therapy: design considerations and clinical applications. Curr Opin Pharmacol 18:18–27. doi: 10.1016/j.coph.2014.08.002

Jirakova K, Seneklova M, Jirak D, Turnovcova K, Vosmanska M, Babic M, et al. The effect of magnetic nanoparticles on neuronal differentiation of induced pluripotent stem cell-derived neural precursors. Int J Nanomedicine. 2016;11:6267-81. Epub 2016/12/07. doi: 10.2147/IJN.S116171.

Jones J, Estirado A, Redondo C, Pacheco-Torres J, Sirerol-Piquer MS, Garcia-Verdugo JM, Martinez S “Mesenchymal stem cells improve motor functions and decrease

neurodegeneration in ataxic mice". Mol Ther. 2014 Jul 29. doi: 10.1038/mt.2014.143.

Jordan A, Scholz R, Maier-Hauff K, van Landeghem FK, Waldoefner N, Teichgraeber U, et al. The effect of thermotherapy using magnetic nanoparticles on rat malignant glioma. J Neurooncol. 2006;78(1):7-14. Epub 2005/11/30. doi: 10.1007/s11060-005-9059-z.

Josephson L, Tung CH, Moore A, Weissleder R (1999) High-efficiency intracellular magnetic labeling with novel superparamagnetic-Tat peptide conjugates. Bioconjug Chem 10:186–191. doi: 10.1021/bc980125h

Kafshgari MH, Harding FJ, Voelcker NH (2015) Insights into cellular uptake of nanoparticles. Curr Drug Deliv 12:63–77

Kallur T, Farr TD, Bohm-Sturm P, Kokaia Z, Hoehn M. Spatio-temporal dynamics, differentiation and viability of human neural stem cells after implantation into neonatal rat brain. Eur J Neurosci. 2011;34(3):382-93. Epub 2011/06/29. doi: 10.1111/j.1460-9568.2011.07759.x.

Kaminski M, Bechmann I, Kiwit J, Glumm J. Migration of monocytes after intracerebral injection. Cell Adh Migr. 2012 May-Jun;6(3):164-7. doi: 10.4161/cam.20281.

Karussis D, Karageorgiou C, Vaknin-Dembinsky A, et al (2010) Safety and immunological effects of mesenchymal stem cell transplantation in patients with multiple sclerosis and amyotrophic lateral sclerosis. Arch Neurol 67:1187–1194. doi: 10.1001/archneurol.2010.248.

Kehrer JP (2000) The Haber-Weiss reaction and mechanisms of toxicity. Toxicology 149:43–50

Khan MI, Mohammad A, Patil G, et al (2012) Induction of ROS, mitochondrial damage and autophagy in lung epithelial cancer cells by iron oxide nanoparticles. Biomaterials 33:1477–1488. doi: 10.1016/j.biomaterials.2011.10.080

Kim D, Chun B-G, Kim Y-K, et al (2008) In vivo tracking of human mesenchymal stem cells in experimental stroke. Cell Transplant 16:1007–1012

Kinney JH, Nichols MC. X-ray tomographic microscopy (XTM) using synchrotron radiation. Ann Rev Mater Sci 1992; 22: 121–52.

Kong S.D., Lee J., Ramachandran S., Eliceiri B.P., Shubayev V.I., Lal R., Jin S. Magnetic targeting of nanoparticles across the intact blood-brain barrier. J. Control. Release. 2012;164:49–57. doi: 10.1016/j.jconrel.2012.09.021.

Kostura L, Kraitchman DL, Mackay AM, et al (2004) Feridex labeling of mesenchymal stem cells inhibits chondrogenesis but not adipogenesis or osteogenesis. NMR Biomed 17:513–517. doi: 10.1002/nbm.925

Kraitchman DL, Heldman AW, Atalar E, et al (2003) In Vivo Magnetic Resonance Imaging of Mesenchymal Stem Cells in Myocardial Infarction. Circulation 107:2290–2293. doi: 10.1161/01.CIR.0000070931.62772.4E

Kralj S, Rojnik M, Romih R, et al (2012) Effect of surface charge on the cellular uptake of fluorescent magnetic nanoparticles. J Nanoparticle Res 14:1151. doi: 10.1007/s11051-012-1151-7

Kuhn et al (2014) Different endocytotic uptake mechanisms for nanoparticles in epithelial cells and macrophages. Beilstein J Nanotechnol. 5: 1625–1636. doi: 10.3762/bjnano.5.174

Kumar M, Singh G, Arora V, et al (2012) Cellular interaction of folic acid conjugated superparamagnetic iron oxide nanoparticles and its use as contrast agent for targeted magnetic imaging of tumor cells. Int J Nanomedicine 7:3503–3516. doi: 10.2147/IJN.S32694

Küstermann et al. (2008) Efficient stem cell labeling for MRI studies. Contrast Media & Molecular Imaging 3:27-37. doi.org/10.1002/cmmi.229

Landry R, Jacobs PM, Davis R, et al (2005) Pharmacokinetic study of ferumoxytol: a new iron replacement therapy in normal subjects and hemodialysis patients. Am J Nephrol 25:400–410. doi: 10.1159/000087212

Laskar A, Ghosh M, Khattak SI, et al (2012) Degradation of superparamagnetic iron oxide nanoparticle-induced ferritin by lysosomal cathepsins and related immune response. Nanomed 7:705–717. doi: 10.2217/nnm.11.148

Laurent S, Forge D, Port M, et al (2008) Magnetic Iron Oxide Nanoparticles: Synthesis, Stabilization, Vectorization, Physicochemical Characterizations, and Biological Applications. Chem Rev 108:2064–2110. doi: 10.1021/cr068445e

Lee JH, Huh YM, Jun YW, Seo JW, Jang JT, Song HT, Kim S, Cho EJ, Yoon HG, Suh JS, Cheon J. Artificially engineered magnetic nanoparticles for ultra-sensitive molecular imaging. Nat Med. 2007 Jan;13(1):95-9.

Lévy M, Lagarde F, Maraloiu V-A, et al (2010) Degradability of superparamagnetic nanoparticles in a model of intracellular environment: follow-up of magnetic, structural and chemical properties. Nanotechnology 21:395103. doi: 10.1088/0957-4484/21/39/395103

Lewin M, Carlesso N, Tung CH, et al (2000) Tat peptide-derivatized magnetic nanoparticles allow in vivo tracking and recovery of progenitor cells. Nat Biotechnol 18:410–414. doi: 10.1038/74464

Li L, Jiang W, Luo K, et al (2013) Superparamagnetic Iron Oxide Nanoparticles as MRI contrast agents for Non-invasive Stem Cell Labeling and Tracking. Theranostics 3:595–615. doi: 10.7150/thno.5366

Li, S.C.;Tachiki,L.M.L.;Luo,J.;Dethlefs,B.A.;Chen,Z.; Loudon, W. G. A biological global positioning system: Considerations for tracking stem cell behaviors in the whole body. Stem Cell Rev. 6(2):317–333; 2010.

Lindvall O, Kokaia Z. Stem cells for the treatment of neurological disorders. Nature. 2006;441(7097):1094-6. Epub 2006/07/01. doi: 10.1038/nature04960.

Liu D, Wu W, Ling J, et al (2011) Effective PEGylation of Iron Oxide Nanoparticles for High Performance In Vivo Cancer Imaging. Adv Funct Mater 21:1498–1504. doi: 10.1002/adfm.201001658

Liu G, Men P, Perry G, Smith MA (2010) Nanoparticle and iron chelators as a potential novel Alzheimer therapy. Methods Mol Biol Clifton NJ 610:123–144. doi: 10.1007/978-1-60327-029-8_8

Liu Z, Li Y, Zhang X, Savant-Bhonsale S, Chopp M. Contralesional axonal remodeling of the corticospinal system in adult rats after stroke and bone marrow stromal cell treatment. Stroke. 2008;39(9):2571-7. Epub 2008/07/12. doi: 10.1161/STROKEAHA.107.511659.

Lojk J, Bregar VB, Rajh M, et al (2015) Cell type-specific response to high intracellular loading of polyacrylic acid-coated magnetic nanoparticles. Int J Nanomedicine 10:1449–1462. doi: 10.2147/IJN.S76134

Long, C. M.; Bulte, J. W. In vivo tracking of cellular therapeutics using magnetic resonance imaging. Expert Opin. Biol. Ther. 9(3):293–306; 2009.

Lu LJ, Wang Y, Cao MH, Chen MW, Lin BL, Duan XH, et al. A novel polymeric micelle used for in vivo MR imaging tracking of neural stem cells in acute ischemic stroke. Rsc Advances. 2017;7(25):15041-52. doi: 10.1039/c7ra00345e.

Lundqvist M, Stigler J, Elia G, Lynch I, Cedervall T, Dawson KA (2008) Nanoparticle size and surface properties determine the protein corona with possible implications for biological impacts. Proc Natl Acad Sci U S A. 105(38):14265-70. doi: 10.1073/pnas.0805135105.

Lunov O, Syrovets T, Büchele B, et al (2010a) The effect of carboxydextran-coated superparamagnetic iron oxide nanoparticles on c-Jun N-terminal kinase-mediated apoptosis in human macrophages. Biomaterials 31:5063–5071. doi: 10.1016/j.biomaterials.2010.03.023

Lunov O, Syrovets T, Röcker C, et al (2010) Lysosomal degradation of the carboxydextran shell of coated superparamagnetic iron oxide nanoparticles and the

fate of professional phagocytes. Biomaterials 31:9015–9022. doi: 10.1016/j.biomaterials.2010.08.003

Lunov O, Zablotskii V, Syrovets T, et al (2011) Modeling receptor-mediated endocytosis of polymer-functionalized iron oxide nanoparticles by human macrophages. Biomaterials 32:547–555. doi: 10.1016/j.biomaterials.2010.08.111

Luo L, Nishi K, Urata Y, Yan C, Hasan AS, Goto S, Kudo T, Li ZL, and Li TS. Ionizing Radiation Impairs Endogenous Regeneration of Infarcted Heart: An In Vivo 18F-FDG PET/CT and 99mTc-Tetrofosmin SPECT/CT Study in Mice. Radiation Research Jan 2017 : Vol. 187, Issue 1 89- 97

Malloy KE, Li J, Choudhury GR, Torres A, Gupta S, Kantorak C, et al. Magnetic Resonance Imaging-Guided Delivery of Neural Stem Cells into the Basal Ganglia of Nonhuman Primates Reveals a Pulsatile Mode of Cell Dispersion. Stem Cells Transl Med. 2017;6(3):877-85. Epub 2017/03/16. doi: 10.5966/sctm.2016-0269.

Malvindi MA, De Matteis V, Galeone A, et al (2014) Toxicity assessment of silica coated iron oxide nanoparticles and biocompatibility improvement by surface engineering. PloS One 9:e85835. doi: 10.1371/journal.pone.0085835

Mani V, Adler E, Briley-Saebo KC, et al (2008) Serial in vivo positive contrast MRI of iron oxide-labeled embryonic stem cell-derived cardiac precursor cells in a mouse model of myocardial infarction. Magn Reson Med 60:73–81. doi: 10.1002/mrm.21642

Marinescu, M., Langer, M., Durand, A., Olivier, C., Chabrol, A., Rositi, H., Chaveau, F., Cho, T., Nighoghossian, N., Berthezène, Y., Peyrin, F., Wiart, M., 2013. Synchrotron radiation x-ray phase microcomputed tomography as a new method to detect iron oxide nanoparticles in the brain. Molecular Imaging and Biology 15, 552-559.

Markides H, Kehoe O, Morris RH, El Haj AJ. (2013) Whole body tracking of superparamagnetic iron oxide nanoparticle-labelled cells – a rheumatoid arthritis mouse model. Stem Cell Res Ther. 4(5): 126.

Martin RM, Leonhardt H, Cardoso MC (2005) DNA labeling in living cells. Cytometry A. 2005 Sep;67(1):45-52.

Masserini M (2013) Nanoparticles for Brain Drug Delivery
ISRN Biochem. 2013; 2013: 238428. Published online 2013 May 21. doi: 10.1155/2013/238428 PMCID: PMC4392984

McAteer MA, Schneider JE, Ali ZA, et al (2008) Magnetic Resonance Imaging of Endothelial Adhesion Molecules in Mouse Atherosclerosis Using Dual-Targeted Microparticles of Iron Oxide. Arterioscler Thromb Vasc Biol 28:77–83. doi: 10.1161/ATVBAHA.107.145466

Miltenyi S, Muller W, Weichel W, Radbruch A. High gradient magnetic cell separation with MACS. Cytometry. 1990;11(2):231-8. doi: 10.1002/cyto.990110203.

Mochizuki H, Yasuda T (2012) Iron accumulation in Parkinson's disease. J Neural Transm Vienna Austria 1996 119:1511–1514. doi: 10.1007/s00702-012-0905-9

Modo M, Beech JS, Meade TJ, Williams SC, Price J. A chronic 1 year assessment of MRI contrast agent-labelled neural stem cell transplants in stroke. Neuroimage. 2009;47 Suppl 2:T133-42. Epub 2008/07/19. doi: 10.1016/j.neuroimage.2008.06.017.

Modo M, Hoehn M, Bulte JW. Cellular MR imaging. Mol Imaging. 2005;4(3):143-64. Epub 2005/10/01.

Modo M, Mellodew K, Cash D, Fraser SE, Meade TJ, Price J, et al. Mapping transplanted stem cell migration after a stroke: a serial, in vivo magnetic resonance imaging study. Neuroimage. 2004;21(1):311-7. Epub 2004/01/27.

Moghimi SM, Andersen AJ, Hashemi SH, et al (2010) Complement activation cascade triggered by PEG–PL engineered nanomedicines and carbon nanotubes: The challenges ahead. J Controlled Release 146:175–181. doi: 10.1016/j.jconrel.2010.04.003

Monnier CA, Burnand D, Rothen-Rutishauser B, Lattuada M, Petri-Fink A (2014) Magnetoliposomes: opportunities and challenges European Journal of Nanomedicine 6(4). doi.org/10.1515/ejnm-2014-0042

Muja N, Bulte JW. Magnetic resonance imaging of cells in experimental disease models. Prog Nucl Magn Reson Spectrosc. 2009;55(1):61-77. Epub 2009/07/01. doi: 10.1016/j.pnmrs.2008.11.002.

Muñoz Y, Carrasco CM, Campos JD, Aguirre P, Núñez MT. Parkinson's Disease: The Mitochondria-Iron Link. Parkinsons Dis. 2016; 2016: 7049108. Published online 2016 May 17. doi: 10.1155/2016/7049108

Naumova AV, Modo M, Moore A, Murry CE, Frank JA. Clinical imaging in regenerative medicine. Nat Biotechnol. 2014;32(8):804-18. Epub 2014/08/06. doi: 10.1038/nbt.2993.

NDong C, Tate JA, Kett WC, et al (2015) Tumor Cell Targeting by Iron Oxide Nanoparticles Is Dominated by Different Factors In Vitro versus In Vivo. PLOS ONE 10:e0115636. doi: 10.1371/journal.pone.0115636

Neri M, Maderna C, Cavazzin C, et al (2008) Efficient in vitro labeling of human neural precursor cells with superparamagnetic iron oxide particles: relevance for in vivo cell tracking. Stem Cells Dayt Ohio 26:505–516. doi: 10.1634/stemcells.2007-0251

Nguyen PK, Riegler J, Wu JC. Stem cell imaging: from bench to bedside. Cell Stem Cell. 2014 Apr 3;14(4):431-44

Ni F, Jiang L, Yang R, et al (2012) Effects of PEG length and iron oxide nanoparticles size on reduced protein adsorption and non-specific uptake by macrophage cells. J Nanosci Nanotechnol 12:2094–2100

Nkansah, M. K.; Thakral, D.; Shapiro, E. M. Magnetic poly(lactide-co-glycolide) and cellulose particles for MRI-based cell tracking. Magn. Reson. Med. 65(6):1776–1785; 2011.

Norman AB, Thomas SR, Pratt RG, Lu SY, Norgren RB. Magnetic resonance imaging of neural transplants in rat brain using a superparamagnetic contrast agent. Brain Res. 1992;594(2):279-83. PubMed PMID: 1450953.

Núñez MT, Urrutia P, Mena N, et al (2012) Iron toxicity in neurodegeneration. Biometals Int J Role Met Ions Biol Biochem Med 25:761–776. doi: 10.1007/s10534-012-9523-0

Odintsov B, Chun JL, Berry SE. Whole body MRI and fluorescent microscopy for detection of stem cells labeled with superparamagnetic iron oxide (SPIO) nanoparticles and DiI following intramuscular and systemic delivery. Methods Mol Biol. 2013;1052:177-93. doi: 10.1007/7651_2013_13.

Pankhurst QA, Connolly J, Jones SK, Dobson J (2003) Applications of magnetic nanoparticles in biomedicine. J Phys Appl Phys 36:R167. doi: 10.1088/0022-3727/36/13/201

Parhamifar L, Larsen AK, Hunter AC, et al (2010) Polycation cytotoxicity: a delicate matter for nucleic acid therapy—focus on polyethylenimine. Soft Matter 6:4001–4009. doi: 10.1039/C000190B

Park E-J, Choi D-H, Kim Y, et al (2014) Magnetic iron oxide nanoparticles induce autophagy preceding apoptosis through mitochondrial damage and ER stress in RAW264.7 cells. Toxicol Vitro Int J Publ Assoc BIBRA 28:1402–1412. doi: 10.1016/j.tiv.2014.07.010

Parton RG, del Pozo MA (2013) Caveolae as plasma membrane sensors, protectors and organizers. Nat Rev Mol Cell Biol 14:98–112. doi: 10.1038/nrm3512

Pavlin M, Bregar VB (2012) Stability of nanoparticle suspensions in different biologically relevant media. Digest Journal of Nanomaterials and Biostructures 7(4):1389-1400

Petters C, Bulcke F, Thiel K, et al (2014) Uptake of fluorescent iron oxide nanoparticles by oligodendroglial OLN-93 cells. Neurochem Res 39:372–383. doi: 10.1007/s11064-013-1234-6

Peng YK, Lui CN, Lin TH, Chang C, Chou PT, Yung KK, et al. Multifunctional silica-coated iron oxide nanoparticles: a facile four-in-one system for in situ study of neural stem cell harvesting. Faraday Discuss. 2014;175:13-26. Epub 2014/10/31. doi: 10.1039/c4fd00132j.

Petters C, Dringen R (2015) Accumulation of iron oxide nanoparticles by cultured primary neurons. Neurochem Int 81:1–9. doi: 10.1016/j.neuint.2014.12.005

Pirko I, Johnson A, Ciric B, Gamez J, Macura SI, Pease LR, Rodriguez M. In vivo magnetic resonance imaging of immune cells in the central nervous system with superparamagnetic antibodies. FASEB J. 2004;18(1):179-82.

Politi LS, Bacigaluppi M, Brambilla E, Cadioli M, Falini A, Comi G, et al. Magnetic-resonance-based tracking and quantification of intravenously injected neural stem cell accumulation in the brains of mice with experimental multiple sclerosis. Stem Cells. 2007;25(10):2583-92. Epub 2007/06/30. doi: 10.1634/stemcells.2007-0037.

Pongrac IM, Pavičić I, Milić M, et al (2016) Oxidative stress response in neural stem cells exposed to different superparamagnetic iron oxide nanoparticles. Int J Nanomedicine 11:1701–1715. doi: 10.2147/IJN.S102730

Pouliquen D, Le Jeune JJ, Perdrisot R, et al (1991) Iron oxide nanoparticles for use as an MRI contrast agent: pharmacokinetics and metabolism. Magn Reson Imaging 9:275–283

Qiao R, Jia Q, Hüwel S, et al (2012) Receptor-Mediated Delivery of Magnetic Nanoparticles across the Blood–Brain Barrier. ACS Nano 6:3304–3310. doi: 10.1021/nn300240p

Qiu B, Xie D, Walczak P, et al (2010) Magnetosonoporation: instant magnetic labeling of stem cells. Magn Reson Med 63:1437–1441. doi: 10.1002/mrm.22348

Radomska A, Leszczyszyn J, Radomski MW.The Nanopharmacology and Nanotoxicology of Nanomaterials: New Opportunities and Challenges. Adv Clin Exp Med. 2016 Jan-Feb;25(1):151-62

Rafatian G, Davis DR1. Heart-Derived Cell Therapy 2.0: Paracrine Strategies to Increase Therapeutic Repair of Injured Myocardium.
Stem Cells. 2018 Sep 1. doi: 10.1002/stem.2910.

Ramos-Cabrer P, Hoehn M. MRI stem cell tracking for therapy in experimental cerebral ischemia. Transl Stroke Res. 2012;3(1):22-35. Epub 2012/03/01. doi: 10.1007/s12975-011-0111-3.

Ramos-Gomez M, Martinez-Serrano A. Tracking of iron-labeled human neural stem cells by magnetic resonance imaging in cell replacement therapy for Parkinson's disease. Neural Regen Res. 2016;11(1):49-52. Epub 2016/03/17. doi: 10.4103/1673-5374.169628.

Ramos-Gómez M, Seiz EG, Martínez-Serrano A (2015) Optimization of the magnetic labeling of human neural stem cells and MRI visualization in the hemiparkinsonian rat brain. J Nanobiotechnology 13:. doi: 10.1186/s12951-015-0078-4.

Rao DB, Wong BA, McManus BE, et al (2003) Inhaled iron, unlike manganese, is not transported to the rat brain via the olfactory pathway. Toxicol Appl Pharmacol 193:116–126. doi: 10.1016/S0041-008X(03)00340-5

Raynal I, Prigent P, Peyramaure S, et al (2004) Macrophage endocytosis of superparamagnetic iron oxide nanoparticles: mechanisms and comparison of ferumoxides and ferumoxtran-10. Invest Radiol 39:56–63. doi: 10.1097/01.rli.0000101027.57021.28

Richards JM, Shaw CA, Lang NN, Williams MC, Semple SI, MacGillivray TJ, Gray C, Crawford JH, Alam SR, Atkinson AP, Forrest EK, Bienek C, Mills NL, Burdess A, Dhaliwal K, Simpson AJ, Wallace WA, Hill AT, Roddie PH, McKillop G, Connolly TA, Feuerstein GZ, Barclay GR, Turner ML, Newby DE. In vivo mononuclear cell tracking using superparamagnetic particles of iron oxide: feasibility and safety in humans. Circ Cardiovasc Imaging. 2012 Jul;5(4):509-17

Rivet CJ, Yuan Y, Borca-Tasciuc D-A, Gilbert RJ (2012) Altering iron oxide nanoparticle surface properties induce cortical neuron cytotoxicity. Chem Res Toxicol 25:153–161. doi: 10.1021/tx200369s

Rojas JM, Sanz-Ortega L, Mulens-Arias V, et al (2016) Superparamagnetic iron oxide nanoparticle uptake alters M2 macrophage phenotype, iron metabolism, migration and invasion. Nanomedicine Nanotechnol Biol Med 12:1127–1138. doi: 10.1016/j.nano.2015.11.020

Rossini A, et al. (2011) Human cardiac and bone marrow stromal cells exhibit distinctive properties related to their origin. Cardiovasc Res. 89(3):650-60. doi: 10.1093/cvr/cvq290.

Sabella S, P. Carney R, Brunetti V, et al (2014) A general mechanism for intracellular toxicity of metal-containing nanoparticles. Nanoscale 6:7052–7061. doi: 10.1039/C4NR01234H

Safi M, Courtois J, Seigneuret M, Conjeaud H, Berret JF (2011) The effects of aggregation and protein corona on the cellular internalization of iron oxide nanoparticles. Biomaterials. 32(35):9353-63. doi: 10.1016/j.biomaterials.2011.08.048.

Saiyed, Z., Gandhi, N., and Nair, M. P. N. (2010) Magnetic nanoformulation of azidothymidine 5-triphosphate for targeted delivery across the blood-brain barrier. Int. J. Nanomed. 5, 157−166.

Sakhtianchi R, Minchin RF, Lee K-B, et al (2013) Exocytosis of nanoparticles from cells: Role in cellular retention and toxicity. Adv Colloid Interface Sci 201–202:18–29. doi: 10.1016/j.cis.2013.10.013

Scharlach C, Müller L, Wagner S, Kobayashi Y, Kratz H, Ebert M, Jakubowski N, Schellenberger E. LA-ICP-MS Allows Quantitative Microscopy of Europium-Doped Iron Oxide Nanoparticles and is a Possible Alternative to Ambiguous Prussian Blue Iron Staining. J Biomed Nanotechnol. 2016 May;12(5):1001-10.

Selt M1, Tennstaedt A1, Beyrau A1, Nelles M1, Schneider G1, Löwik C2, Hoehn M1,2,3. In Vivo Non-Invasive Tracking of Macrophage Recruitment to Experimental Stroke. PLoS One. 2016 Jun 24;11(6):e0156626. doi: 10.1371/journal.pone.0156626. eCollection 2016.

Serrano-Puebla A, Boya P (2016) Lysosomal membrane permeabilization in cell death: new evidence and implications for health and disease. Ann N Y Acad Sci 1371:30–44. doi: 10.1111/nyas.12966

Shapiro EM, Medford-Davis LN, Fahmy TM, Dunbar CE, Koretsky AP (2007) Antibody-mediated cell labeling of peripheral T cells with micron-sized iron oxide particles (MPIOs) allows single cell detection by MRI. Contrast Media Mol Imaging. 2(3):147-53.

Shapiro EM. Biodegradable, polymer encapsulated, metal oxide particles for MRI-based cell tracking. Magn Reson Med. 2015 Jan;73(1):376-89.

Shapiro EM, Sharer K, Skrtic S, Koretsky AP (2006) In vivo detection of single cells by MRI. Magn Reson Med. 2006 Feb;55(2):242-9.

Sharif F, Bartunek J, Vanderheyden M. Adult stem cells in the treatment of acute myocardial infarction. Catheter Cardiovasc Interv. 2011 Jan 1;77(1):72-83).

Sharma HS (2009) Blood–Central Nervous System Barriers: The Gateway to Neurodegeneration, Neuroprotection and Neuroregeneration. In: Handbook of Neurochemistry and Molecular Neurobiology. Springer, Boston, MA, pp 363–457

Shen T, Weissleder R, Papisov M, Bogdanov A Jr, Brady TJ (1993) Monocrystalline iron oxide nanocompounds (MION): physicochemical properties. Magn Reson Med. (5):599-604.

Shen TT, Bogdanov A Jr, Bogdanova A, Poss K, Brady TJ, Weissleder R. (1996) Magnetically labeled secretin retains receptor affinity to pancreas acinar cells. Bioconjug Chem. 7(3):311-6.

Shen W-B, Plachez C, Chan A, et al (2013) Human neural progenitor cells retain viability, phenotype, proliferation, and lineage differentiation when labeled with a novel iron oxide nanoparticle, Molday ION Rhodamine B. Int J Nanomedicine 8:4593–4600. doi: 10.2147/IJN.S53012

Shubayev VI, Thomas R. Pisanic, II, Sungho Jin. Magnetic nanoparticles for theragnostics. Adv Drug Deliv Rev. 2009 Jun 21; 61(6): 467–477. doi: 10.1016/j.addr.2009.03.007

Sitaram M. Emani, Pedro J. del Nido Cell-Based Therapy With Cardiosphere-Derived Cardiocytes A New Hope for Pediatric Patients With Single Ventricle Congenital Heart Disease? Circ Res. 2018;122:916-917

Srivastava AK1, Bulte JW. Seeing stem cells at work in vivo. Stem Cell Rev. 2014 Feb;10(1):127-44. doi: 10.1007/s12015-013-9468-x.

Soenen SJH, Himmelreich U, Nuytten N, et al (2010a) Intracellular nanoparticle coating stability determines nanoparticle diagnostics efficacy and cell functionality. Small Weinh Bergstr Ger 6:2136–2145. doi: 10.1002/smll.201000763

Soenen SJH, Himmelreich U, Nuytten N, De Cuyper M (2011) Cytotoxic effects of iron oxide nanoparticles and implications for safety in cell labelling. Biomaterials 32:195–205. doi: 10.1016/j.biomaterials.2010.08.075

Soenen SJH, Nuytten N, De Meyer SF, et al (2010b) High intracellular iron oxide nanoparticle concentrations affect cellular cytoskeleton and focal adhesion kinase-mediated signaling. Small Weinh Bergstr Ger 6:832–842. doi: 10.1002/smll.200902084

Soenen SJH, Vercauteren D, Braeckmans K, et al (2009) Stable Long-Term Intracellular Labelling with Fluorescently Tagged Cationic Magnetoliposomes. ChemBioChem 10:257–267. doi: 10.1002/cbic.200800510

Steinberg GK, Kondziolka D, Wechsler LR, Lunsford LD, Coburn ML, Billigen JB, et al. Clinical Outcomes of Transplanted Modified Bone Marrow-Derived Mesenchymal Stem Cells in Stroke: A Phase 1/2a Study. Stroke. 2016;47(7):1817-24. Epub 2016/06/04. doi: 10.1161/STROKEAHA.116.012995. PubMed PMID: 27256670.

Stern ST, Adiseshaiah PP/SPP, Crist RM (2012) Autophagy and lysosomal dysfunction as emerging mechanisms of nanomaterial toxicity. Part Fibre Toxicol 9:20. doi: 10.1186/1743-8977-9-20

Stroh A, Faber C, Neuberger T, Lorenz P, Sieland K, Jakob PM, Webb A, Pilgrimm H, Schober R, Pohl EE, Zimmer C. In vivo detection limits of magnetically labeled embryonic stem cells in the rat brain using high-field (17.6 T) magnetic resonance imaging. Neuroimage. 2005;24(3):635-45.

Suarez S, A. Almutairi, and K. L. Christman. Micro- and Nanoparticles for Treating Cardiovascular Disease. Biomater Sci. 2015 Apr 1; 3(4): 564–580. doi: [10.1039/C4BM00441H]

Sumner J, Conroy R, Shapiro E, Moreland J, Koretsky AP. (2007) Delivery of fluorescent probes using iron oxide particles as carriers enables in

vivo labeling of migrating neural precursors for MRI and optical imaging. J Biomed Opt; 12(5):051504.

Szebeni J, Baranyi L, Sávay S, et al (2006) Complement activation-related cardiac anaphylaxis in pigs: role of C5a anaphylatoxin and adenosine in liposome-induced abnormalities in ECG and heart function. Am J Physiol Heart Circ Physiol 290:H1050-1058. doi: 10.1152/ajpheart.00622.2005

Tateishi-Yuyama E, Matsubara H, Murohara T, et al. Therapeutic angiogenesis for patients with limb ischaemia by autologous transplantation of bone marrow cells: a pilot study and a randomised controlled trial. Lancet 2002;360:427–435

Taylor A, Herrmann A, Moss D, et al (2014) Assessing the Efficacy of Nano- and Micro-Sized Magnetic Particles as Contrast Agents for MRI Cell Tracking. PLOS ONE 9:e100259. doi: 10.1371/journal.pone.0100259

Tenzer S, Docter D, Kuharev J, Musyanovych A, Fetz V, Hecht R, Schlenk F, Fischer D, Kiouptsi K, Reinhardt C, Landfester K, Schild H, Maskos M, Knauer SK, Stauber RH (2013) Rapid formation of plasma protein corona critically affects nanoparticle pathophysiology. Nat Nanotechnol. 8(10):772-81. doi: 10.1038/nnano.2013.181.

Terrovitis J, Stuber M, Youssef A, et al (2008) Magnetic Resonance Imaging Overestimates Ferumoxide-Labeled Stem Cell Survival After Transplantation in the Heart. Circulation 117:1555–1562. doi: 10.1161/CIRCULATIONAHA.107.732073

Terrovitis JV, Ruckdeschel Smith R and Marbán E. Assessment and Optimization of Cell Engraftment After Transplantation Into the Heart. Circ. Res. 2010;106;479-494

Thomsen LB, T. Linemann, K. M. Pondman, J. Lichota, K. S. Kim, R. J. Pieters, G. M. Visser, T. Moos. Uptake and Transport of Superparamagnetic Iron Oxide Nanoparticles through Human Brain Capillary Endothelial Cells
ACS Chem Neurosci. 2013 Oct 16; 4(10): 1352–1360. Published online 2013 Aug 6. doi: 10.1021/cn400093z

Thu MS, Najbauer J, Kendall SE, et al (2009) Iron Labeling and Pre-Clinical MRI Visualization of Therapeutic Human Neural Stem Cells in a Murine Glioma Model. PLoS ONE 4:. doi: 10.1371/journal.pone.0007218.

Torrente Y, Gavina M, Belicchi M, Fiori F, Komlev V, Bresolin N, Rustichelli F. High-resolution X-ray microtomography for three-dimensional visualization of human stem cell muscle homing. *FEBS Lett*. 2006; 580(24): 5759–5764.

Treuel L, Docter D, Maskos M, Stauber RH (2015) Protein corona – from molecular adsorption to physiological complexity. Beilstein J Nanotechnol 6:857–873. doi: 10.3762/bjnano.6.88

Tu C, Ng TSC, Sohi HK, et al (2011) Receptor-targeted iron oxide nanoparticles for molecular MR imaging of inflamed atherosclerotic plaques. Biomaterials 32:7209–7216. doi: 10.1016/j.biomaterials.2011.06.026

Tuszynski MH, Wang Y, Graham L, McHale K, Gao M, Wu D, Brock J, Blesch A, Rosenzweig ES, Havton LA, Zheng B, Conner JM, Marsala M, Lu P (2014) Neural stem cells in models of spinal cord injury. Exp Neurol. 261:494-500. doi: 10.1016/j.expneurol.2014.07.011.

Urrutia PJ, Mena NP, Núñez MT (2014) The interplay between iron accumulation, mitochondrial dysfunction, and inflammation during the execution step of neurodegenerative disorders. Front Pharmacol. 5: 38. Published online 2014 Mar 10. doi: 10.3389/fphar.2014.00038

Uttara B, Singh AV, Zamboni P, Mahajan R. (2009) Oxidative Stress and Neurodegenerative Diseases: A Review of Upstream and Downstream Antioxidant Therapeutic Options. Curr Neuropharmacol 7:65–74. doi: 10.2174/157015909787602823

Uygur A, Lee RT (2016) Mechanisms of Cardiac Regeneration.Dev Cell. 36(4):362-74. doi: 10.1016/j.devcel.2016.01.018.

Valable S, Barbier EL, Bernaudin M, et al (2008) In vivo MRI tracking of exogenous monocytes/macrophages targeting brain tumors in a rat model of glioma. NeuroImage 40:973–83

van den Bos EJ, Baks T, Moelker AD, et al (2006) Magnetic resonance imaging of haemorrhage within reperfused myocardial infarcts: possible interference with iron oxide-labelled cell tracking? Eur Heart J 27:1620–1626. doi: 10.1093/eurheartj/ehl059

Vellinga MM, Oude Engberink RD, Seewann A, Pouwels PJ, Wattjes MP, van der Pol SM, Pering C, Polman CH, de Vries HE, Geurts JJ, Barkhof F. Pluriformity of inflammation in multiple sclerosis shown by ultra-small iron oxide particle enhancement. Brain. 2008;131(Pt 3):800-7 doi: 10.1093/brain/awn009.

Volatron J, Carn F, Kolosnjaj-Tabi J, et al (2017) Ferritin Protein Regulates the Degradation of Iron Oxide Nanoparticles. Small Weinh Bergstr Ger 13:. doi: 10.1002/smll.201602030

von der Haar K, Lavrentieva A, Stahl F, Scheper T, Blume C. Lost signature: progress and failures in in vivo tracking of implanted stem cells. Appl Microbiol Biotechnol. 2015;99(23):9907-22. Epub 2015/09/17. doi: 10.1007/s00253-015-6965-7.

Walczak P, Kedziorek DA, Gilad AA, et al (2005) Instant MR labeling of stem cells using magnetoelectroporation. Magn Reson Med 54:769–774. doi: 10.1002/mrm.20701

Walczak P, Ruiz-Cabello J, Kedziorek DA, et al (2006) Magnetoelectroporation: improved labeling of neural stem cells and leukocytes for cellular magnetic resonance imaging using a single FDA-approved agent. Nanomedicine Nanotechnol Biol Med 2:89–94. doi: 10.1016/j.nano.2006.01.003

Wang B, Feng WY, Wang M, Shi JW, Zhang F, Ouyang H, Zhao YL, Chai ZF, Huang YY, Xie YN, Wang HF, Wang J (2007) Transport of intranasally instilled fine Fe2O3 particles into the brain: micro-distribution, chemical states, and histopathological observation. Biol Trace Elem Res. 118(3):233-43.

Wang B, Feng W, Zhu M, et al (2008) Neurotoxicity of low-dose repeatedly intranasal instillation of nano- and submicron-sized ferric oxide particles in mice. J Nanoparticle Res 11:41–53. doi: 10.1007/s11051-008-9452-6

Wang B, Wang Q, Chen H, Zhou X, Wang H, Wang H, Zhang J, Feng W (2016) Size-Dependent Translocation Pattern, Chemical and Biological Transformation of Nano- and Submicron-Sized Ferric Oxide Particles in the Central Nervous System. J Nanosci Nanotechnol. 2016 Jun;16(6):5553-61.

Wang G, Chen F, Banda NK, et al (2016) Activation of Human Complement System by Dextran-Coated Iron Oxide Nanoparticles Is Not Affected by Dextran/Fe Ratio, Hydroxyl Modifications, and Crosslinking. Front Immunol 7:418. doi: 10.3389/fimmu.2016.00418

Wang Y, Xu C, Ow H (2013) Commercial Nanoparticles for Stem Cell Labeling and Tracking. Theranostics 3:544–560. doi: 10.7150/thno.5634

Wang YJ (2011) Superparamagnetic iron oxide based MRI contrast agents: Current status of clinical application. Quant Imaging Med Surg. 2011 Dec; 1(1): 35–40. doi: 10.3978/j.issn.2223-4292.2011.08.03.

Wang Z (2014) Caveolae-mediated Delivery of Therapeutic Nanoparticles across Blood-endothelial Barrier. Austin J Anal Pharm Chem. 1(4):1018.

Wang Z, Tiruppathi C, Cho J, et al (2011) Targeting of Nanoparticle-Complexed Drugs across the Vascular Endothelial Barrier via Caveolae. IUBMB Life 63:659–667. doi: 10.1002/iub.485

Wei H, Insin N, Lee J, Han HS, Cordero JM, Liu W, Bawendi MG. (2012) Compact zwitterion-coated iron oxide nanoparticles for biological applications. Nano Lett. 2012 Jan 11;12(1):22-5. doi: 10.1021/nl202721q. Epub 2011 Dec 20.

Weissleder R, Stark DD, Engelstad BL, et al (1989) Superparamagnetic iron oxide: pharmacokinetics and toxicity. AJR Am J Roentgenol 152:167–173. doi: 10.2214/ajr.152.1.167

Wen X, Wang Y, Zhang F, Zhang X, Lu L, Shuai X, et al. In vivo monitoring of neural stem cells after transplantation in acute cerebral infarction with dual-modal MR imaging and optical imaging. Biomaterials. 2014;35(16):4627-35. Epub 2014/03/19. doi: 10.1016/j.biomaterials.2014.02.042.

Winner B, Winkler J. Adult neurogenesis in neurodegenerative diseases.

Cold Spring Harb Perspect Biol. 2015 Apr 1;7(4):a021287. doi: 10.1101/cshperspect.a021287.

Withers, P.J. (2007) X-ray nanotomography. Materials Today 10(12): 26-34.

Wolf-Grosse S, Rokstad AM, Ali S, Lambris JD, Mollnes TE, Nilsen AM, Stenvik J (2017) Iron oxide nanoparticles induce cytokine secretion in a complement-dependent manner in a human whole blood model. International Journal of Nanomedicine 12:3927—3940. doi.org/10.2147/IJN.S136453

Wu H, Yin J-J, Wamer WG, et al (2014) Reactive oxygen species-related activities of nano-iron metal and nano-iron oxides. J Food Drug Anal 22:86–94. doi: 10.1016/j.jfda.2014.01.007

Wu J, Wang C, Sun J, Xue Y (2011) Neurotoxicity of silica nanoparticles: brain localization and dopaminergic neurons damage pathways. ACS Nano 5:4476–4489. doi: 10.1021/nn103530b

Wu X, Tan Y, Mao H, Zhang M (2010) Toxic effects of iron oxide nanoparticles on human umbilical vein endothelial cells. Int J Nanomedicine 5:385–399

Xie D, Qiu B, Walczak P, et al (2010) Optimization of magnetosonoporation for stem cell labeling. NMR Biomed 23:480–484. doi: 10.1002/nbm.1485

Yang T, Sun S, Ma M, Lin Q, Zhang L, Li Y, Luo F (2015) Optimizing immobilization of avidin on surface-modified magnetic nanoparticles: characterization and application of protein-immobilized nanoparticles. Bioprocess and Biosystems Engineering, Volume 38, Issue 10, pp 2023–2034

Yarjanli Z, Ghaedi K, Esmaeili A, et al (2017) Iron oxide nanoparticles may damage to the neural tissue through iron accumulation, oxidative stress, and protein aggregation. BMC Neurosci 18:. doi: 10.1186/s12868-017-0369-9

Yeh TC, Zhang W, Ildstad ST, Ho C (1993) Intracellular labeling of T-cells with superparamagnetic contrast agents. Magn Reson Med Off J Soc Magn Reson Med Soc Magn Reson Med 30:617–625.

Yeh TC, Zhang W, Ildstad ST, Ho C (1995) In vivo dynamic MRI tracking of rat T-cells labeled with superparamagnetic iron-oxide particles. Magn Reson Med 33:200–208

Yilmaz A, Dengler MA, van der Kuip H, Yildiz H, Rösch S, Klumpp S, Klingel K, Kandolf R, Helluy X, Hiller KH, Jakob PM, Sechtem U. Imaging of myocardial infarction using ultrasmall superparamagnetic iron oxide nanoparticles: a human study using a multi-parametric cardiovascular magnetic resonance imaging approach. Eur Heart J. 2013 Feb;34(6):462-75

Yokoyama T, Tam J, Kuroda S, et al (2011) EGFR-Targeted Hybrid Plasmonic Magnetic Nanoparticles Synergistically Induce Autophagy and Apoptosis in Non-Small Cell Lung Cancer Cells. PLOS ONE 6:e25507. doi: 10.1371/journal.pone.0025507

Yuan Z-Y, Hu Y-L, Gao J-Q (2015) Brain Localization and Neurotoxicity Evaluation of Polysorbate 80-Modified Chitosan Nanoparticles in Rats. PLoS One. 10(8): e0134722. doi: 10.1371/journal.pone.0134722

Zhang X, Zhang H, Liang X, et al (2016) Iron Oxide Nanoparticles Induce Autophagosome Accumulation through Multiple Mechanisms: Lysosome Impairment, Mitochondrial Damage, and ER Stress. Mol Pharm 13:2578–2587. doi: 10.1021/acs.molpharmaceut.6b00405

Zhang Z, Jiang Q, Jiang F, et al (2004) In vivo magnetic resonance imaging tracks adult neural progenitor cell targeting of brain tumor. NeuroImage 23:281–287. doi: 10.1016/j.neuroimage.2004.05.019

Zheng B, Vazin T, Goodwill PW, Conway A, Verma A, Saritas EU, et al. Magnetic Particle Imaging tracks the long-term fate of in vivo neural cell implants with high image contrast. Sci Rep. 2015;5:14055. Epub 2015/09/12. doi: 10.1038/srep14055.

Zhu J, Zhou L, XingWu F (2006) Tracking neural stem cells in patients with brain trauma. N Engl J Med. 2006 Nov 30;355(22):2376-8. DOI: 10.1056/NEJMc055304

Zhu K, Li J, Wang Y, Lai H, Wang C (2016) Nanoparticles-Assisted Stem Cell Therapy for Ischemic Heart Disease. Stem Cells Int. 2016:1384658.

Aarntzen EH, Srinivas M, Walczak P, Janowski M, Heerschap A, de Vries IJ, Figdor CG, Bulte JW, Oyen WJ. In vivo tracking techniques for cellular regeneration, replacement, and redirection. J Nucl Med. 2012 Dec;53(12):1825-8. doi: 10.2967/jnumed.112.106146.